REPORT DOCUMENTATION PAGE

Form Approved OMB No. 0704-0188

1. REPORT DATE *(DD-MM-YYYY)* 19-07-2010	2. REPORT TYPE Final Report	3. DATES COVERED *(From – To)* 01-Dec-06 - 19-Jul-10

4. TITLE AND SUBTITLE

Tailoring of microstructure and properties of titanium parts with local rapid heat treatment

5a. CONTRACT NUMBER
STCU Registration No: P-246

5b. GRANT NUMBER

5c. PROGRAM ELEMENT NUMBER

6. AUTHOR(S)

Dr. Pavlo Evgenovich Markovsky

5d. PROJECT NUMBER

5d. TASK NUMBER

5e. WORK UNIT NUMBER

7. PERFORMING ORGANIZATION NAME(S) AND ADDRESS(ES)
G.V Kurdyumov Institute for Metal Physics, National Academy of Sciences of Ukraine
36, Vernadsky Blvd
Kiev 03142
Ukraine

8. PERFORMING ORGANIZATION REPORT NUMBER

N/A

9. SPONSORING/MONITORING AGENCY NAME(S) AND ADDRESS(ES)

EOARD
Unit 4515 BOX 14
APO AE 09421

10. SPONSOR/MONITOR'S ACRONYM(S)

11. SPONSOR/MONITOR'S REPORT NUMBER(S)
STCU 06-8001

12. DISTRIBUTION/AVAILABILITY STATEMENT

Approved for public release; distribution is unlimited.

13. SUPPLEMENTARY NOTES

14. ABSTRACT

This report results from a contract tasking G.V Kurdyumov Institute for Metal Physics, National Academy of Sciences of Ukraine as follows: Proposed project is dedicated to development of physical background of Local Heat Rapid Treatment (LRHT) of titanium parts, which allowed to improve a balance of its mechanical properties (tensile and fatigue). Employing three different commercial titanium alloys as program material research work will consist of two main efforts. The first effort will be a detailed study of dependencies between LRHT regimes (employing testing specimens), obtained 3-D microstructural conditions, and their mechanical properties. The second effort will include checking the applicability of the developed approach for use with real parts, taking as an example titanium compressor blade. As a final result LRHT/microstructure/properties/ maps could be developed for selected titanium alloys.

15. SUBJECT TERMS
EOARD, Materials, Metallurgy and Metallography

16. SECURITY CLASSIFICATION OF:

a. REPORT UNCLAS	b. ABSTRACT UNCLAS	c. THIS PAGE UNCLAS	17. LIMITATION OF ABSTRACT UL	18, NUMBER OF PAGES 49	19a. NAME OF RESPONSIBLE PERSON WYNN SANDERS, Maj, USAF
					19b. TELEPHONE NUMBER *(Include area code)* +44 (0)1895 616 007

Standard Form 298 (Rev. 8/98)
Prescribed by ANSI Std. Z39-18

"Tailoring of microstructure and properties of titanium parts with local rapid heat treatment"

Project manager: Dr. Pavlo E. Markovsky

Tel: (380-44) 424-01-20, Fax (380-44)424-33-74, E-mail pmark@imp.kiev.ua

Kurdyumov Institute for Metal Physics NAS of Ukraine, 36, Vernadsky Blvd, 03142, Kyiv, Ukraine

Content of the Final Report

List of Figures

1. SUMMARY

Performed project was aimed on formation of special unique structural conditions, that are characterized by fine-grained fully beta-transformed microstructure in specific locations (or surface layers), which should cause in achievement of significantly improved balance of mechanical (tensile and fatigue) properties. Experimental works consisted of two main parts. First of them was performed employing as an object cylindrical specimens 8 mm in diameter of three titanium base alloys representing different types of this material: i) alpha-base commercial purity titanium (CP-Ti); ii) "working horse of titanium industry two-phase $\alpha+\beta$ Ti-6(wt.)%Al-4%V alloy; and iii) beta-alloy TIMETAL-LCB. Local (Surface) Rapid Heat Treatment (LRHT) was performed with Electromagnetic Induction heating using developed in this project installation on the base of 440 kHz/ 5kWt induction generator and wide range of specially designed inductors. As a result of systematic study main dependencies of LRHT regime influence on gradient microstructural condition formation in titanium alloys of different types were established and possibility of essential improvement of mechanical properties balance was shown.

Obtained with cylindrical specimens and this approach experimental data allowed us to go to the second part of this project and apply LRHT for treatment of real part – turbine engine compressor blade. As a result, essential improvement of service properties – fatigue performance (including case of stress concentrator appearance), was established for compressor blades subjected to LRHT.

All works were done in complete accordance with specified working plan.

2. INTRODUCTION

Titanium alloys found a wide application in aerospace industry. Mechanical properties of these alloys strongly depend on their phase composition and microstructure formed with thermomechanical processing and bulk heat treatment. However, quite common is a situation when different sections of the same part require different properties. For instance, for dovetail of compressor blades wear resistance as well as fretting behavior are important, while for the other locations of the blades fatigue performance, creep behavior, erosion resistance and impact toughness are critical. Therefore, in order to achieve an optimized part performance, microstructure and phase compositions should be carefully tailored locally while commonly used treatments are some kind of compromise, providing a balance of mechanical properties on a medium level. In the

present project Induction heating was chosen as a method of Local (surface) Rapid Heat Treatment (LRHT) aimed on formation of 3-D gradient microstructure and phase composition fields which should allow to increase reliability and service life of complicated-shape titanium parts.

3. METHODS, ASSUMPTIONS, AND PROCEDURES

Research works in this project included evaluation of macro- and microstructure of materials in initial and heat treated conditions, and were performed using standard methods of Light (LM) and Transition Electron (TEM) Microscopy. Microhardness was measures with standard HB method. Tensile tests were performed using INSTRON-3367 machine with ASTM E8-7 and specimens having 4 mm gage diameter. Fatigue tests for cylindrical specimens were made using hour-glass shaped specimens having 3.8 mm gage diameter in the central part, with rotating beam method; rotation frequency 45 Hz, symmetric cycle, at room temperature. For blades pure banding method was employed, which details will be given in relevant part of this report (see Chapter 4.3).

3.1. Performing of Local Rapid Heat Treatment (LRHT)

Induction heating was employed in this project as a method of local/surface rapid heat treatment (LRHT) [1]. Basing on 5 kWt, 440 kHz generator [2] we designed and made the complex installation (Fig.1) on the base of available 440 kHz 5kWt transistor generator VChI-5 (1) was designed, made and tested. Employed power unit was chosen from the reason to generate heat in a very thin (of about 1.2 mm according to calculations made with given in [3] equations) surface layer.
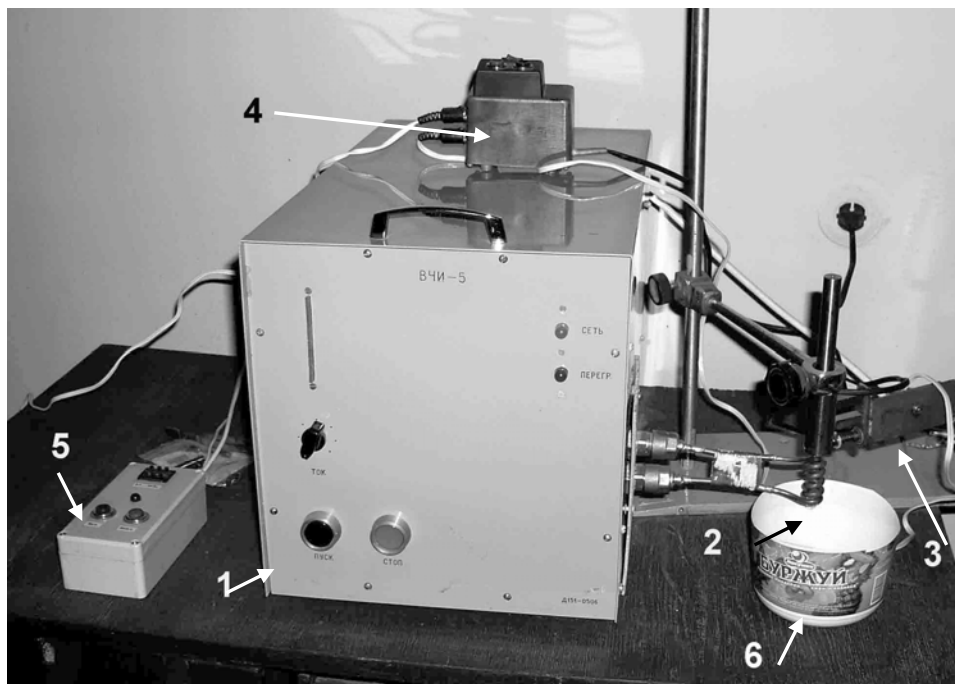
Fig.1. Installation for Local Rapid Heat Treatment (LRHT, induction heating method); (1) – 440 kHz, 5 kWt generator; (2) – inductor for treatment of Ø8 mm cylindrical specimens, (3) – specimens' electromagnetic holder; (4) – specimens' holder control unit (for specimens installation); (5) – control unit for heating and automatic quenching of specimens; (6) – quenching vessel.

This installation includes: inductor for heating of cylindrical specimens (2) or for heating of leading edge of aircraft engine compressor blades (See Fig. 2 in the progress report for the first quarter); specimens' electromagnetic holder (3), which automatically drops specimen after finishing of heating; specimens' holder control unit (4), which is employed for specimens installation; control unit assigning duration of heating with accuracy 0.1 sec (5); and quenching vessel with water (6). Several inductors having different size and shape (Fig. 2) were prepared and tested. On the base of macrostructural data (Fig. 3) the best from the point of view to provide more uniform and smooth thermal front inductor with "one-side flattened" type of cross-section (flat on the inner side of coil) was chosen (Fig. 2e). From presented in Fig.3 macrostructures it is also possible to conclude that changing of type of inductor and level of applied energy allows to vary depth and shape of heated surface layers, as well as smoothness/sharpness of transition zones in specimens.

During testing of this installation several different types of specimens (Fig. 4) were chosen and tested due the necessity to find better way to form beta-transformed surface layers of different thickness. With inductor of one type (with inner diameter 10 mm) efficient heating of specimens can be performed for diameters from 8 to 6 mm only (to be employed for subsequent cutting of tensile and fatigue testing specimens), while for thinner specimens efficiency of energy injection into specimen surface became rather low. Since one of the main goals of present project was to obtain different fraction of LRHT-treated material, Ø 8 mm specimens were used in further study.

It is necessary to underline, that for applied energies of 4 and 5 kWt the whole range of LRHT-treated layers (from 0 up to 100% volume fraction) was formed within very narrow time ranges 2-3 and 3-4 seconds respectively. As for 5 kWt applied power dependences of beta-treated material fraction vs. time for two alloys studied (CPTi and Ti-6-4) are presented in Fig. 5.

Summarizing performed during this activity works it is possible to conclude that required equipment and LRHT approach ensuring formation of conditions having different volume fraction of treated part was developed, that allows us to fulfill estimated goals of this project.
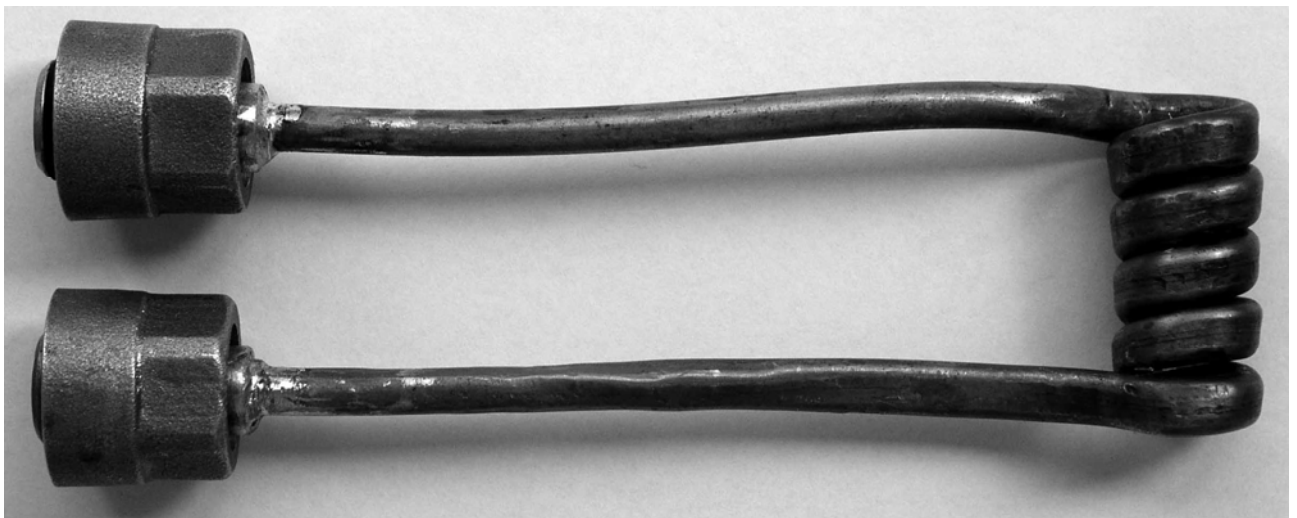
a
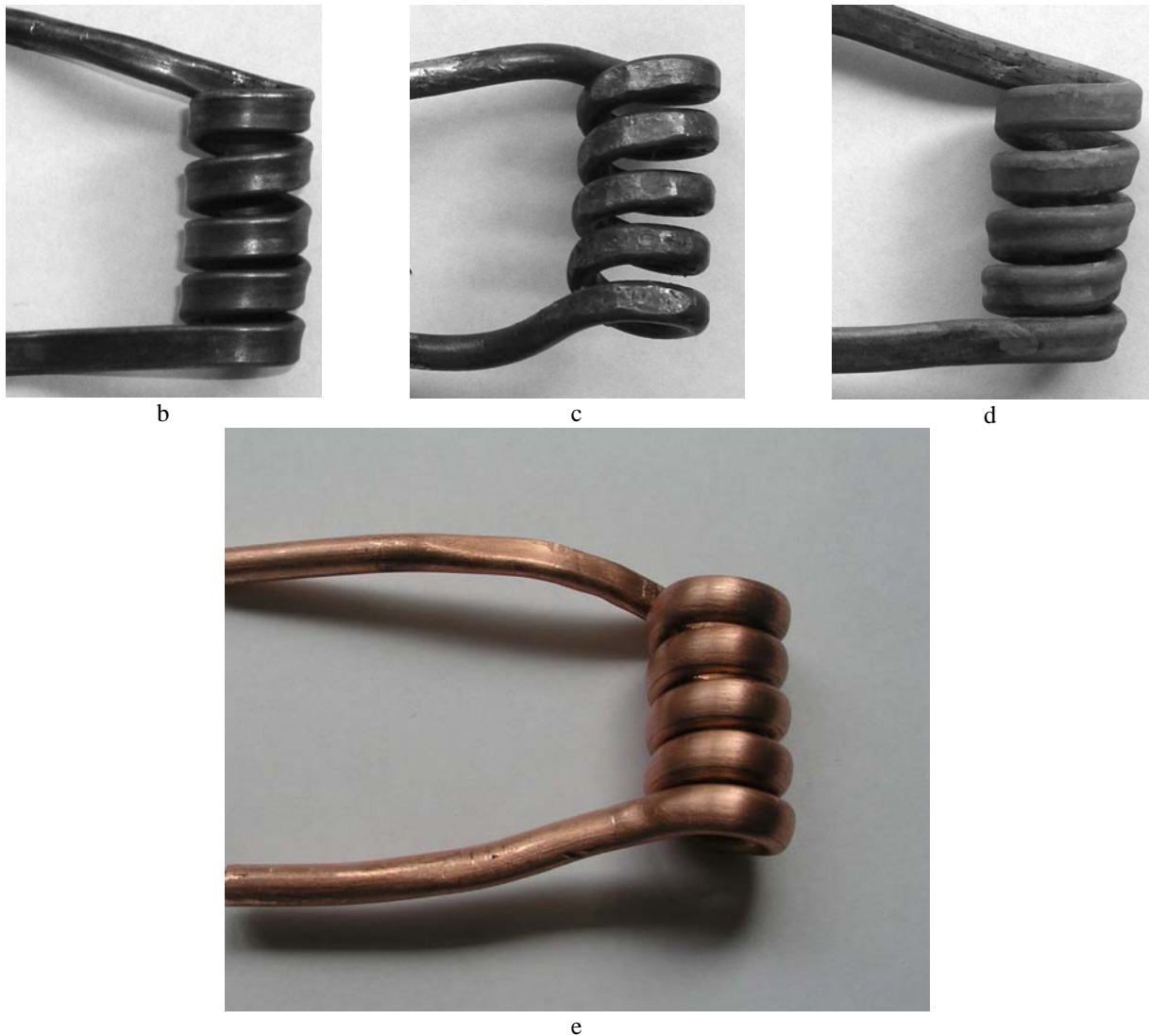
Fig.2 Examples of some made and tested inductors; (a) – Ø 6mm, a.r. 4/7; (b) – Ø 4mm, a.r. 2.5/5; (c) – Ø 5mm, a.r. 4/5.7; (d) – Ø 5 mm, a.r. 3.5/6.1. e - operating part of more efficient inductor (Ø 5mm) having one-side (inner) flattened cross-section in coil part.

c

d

4 mm

e
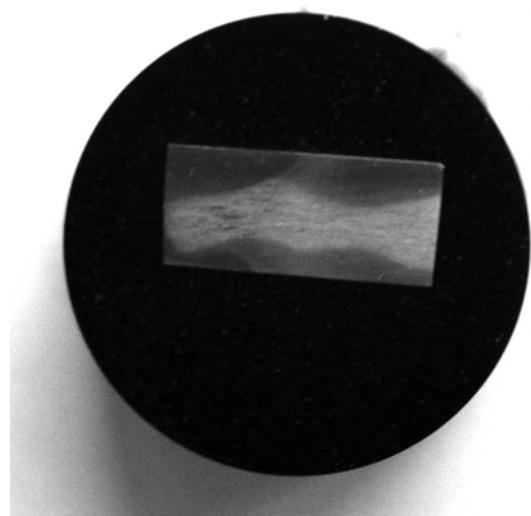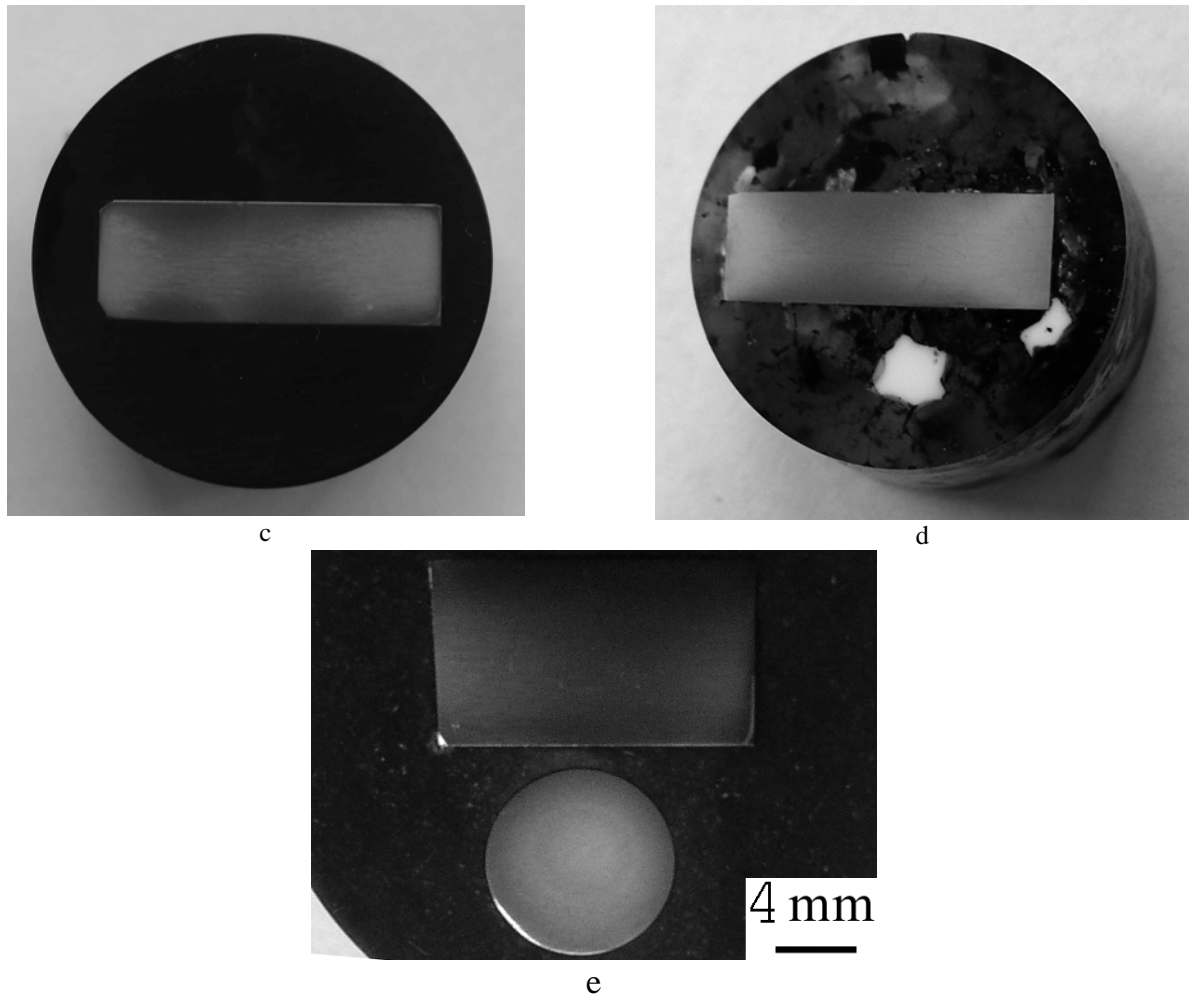
Fig.3 Comparison of macrostructure of CP-Ti obtained using different kind of inductors: (a) – initial one having round cross-section Ø 5mm, a.r. 3.5/6; (b) - Ø 5mm, a.r. 4/5.7; (c) - Ø 6mm, a.r. 4/7; (d, e) - Ø 5mm, flattened from one side. Applied energy: (a-c) 5 kWt; (d, e) 4 kWt.
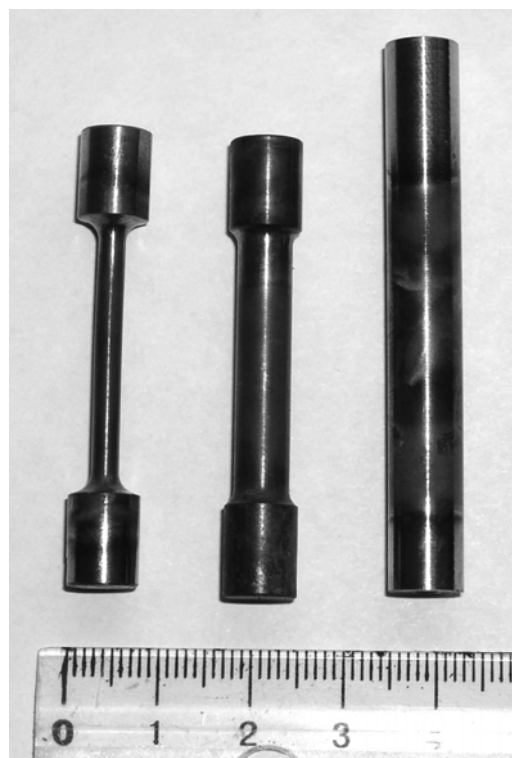
Fig. 4. Examples of different types of specimens tested.
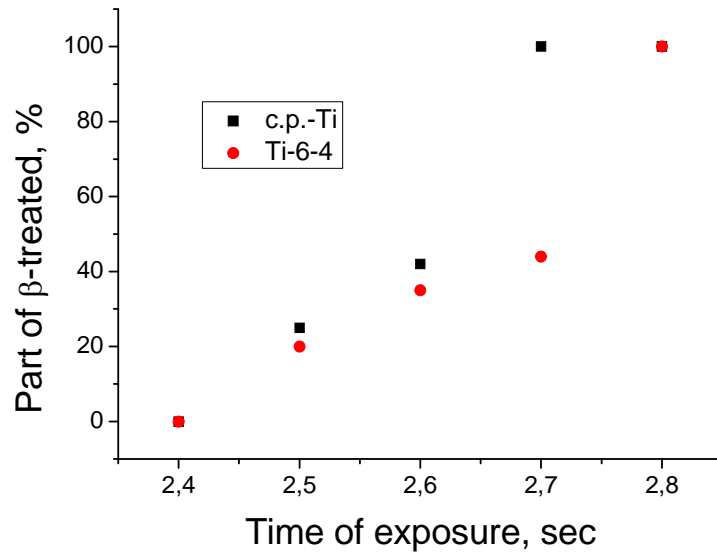
Fig. 5 Influence of induction heating (5 kWt) duration on the relative thickness of treated layers.

For LRHT of real turbine engine compressor blades special loop inductor for leading edge treatment (Fig. 6a) and for LRHT of convex face (Fig. 6b) were designed and made.

a
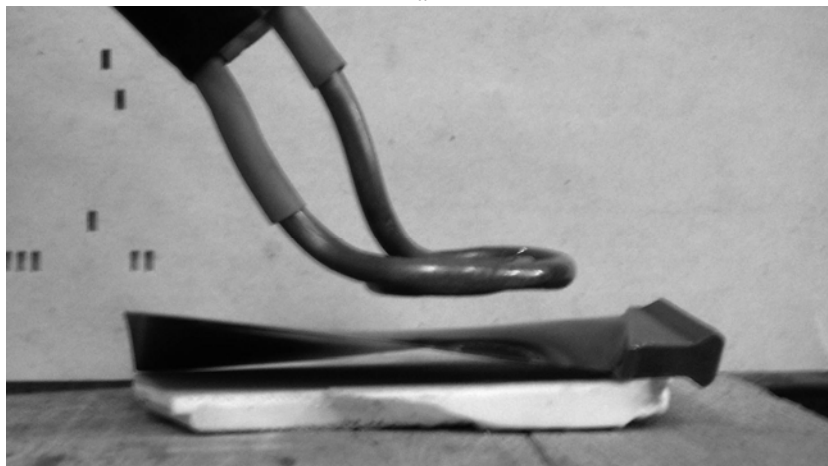
b

Fig.6. General view of inductors for LRHT of compressor blades: (a) – for LRHT of leading edge, (b) – for LRHT of convex face.

3.2. Measurement of residual stresses in CP-Ti

Since obtained on the beginning of the project results for mechanical properties of CP-Ti after LRHT could not be explained with microstructure changes only, it was supposed, that some influence may be attributed to appearance during very fast heating and cooling of residual stresses. That is why we made an attempt to evaluate qualitatively the residual stresses developed in specimens after LRHT and water quenching. Estimation of stresses accumulated in complicated (not flat) shape parts, especially having gradient in microstructure, defects distribution, etc. is very complicated problem. Known X-Ray methods of residual stresses evaluation are well developed and rather accurate in case of investigation of objects having flat surface [4-5]. In this case estimated common stress σ is a sum of main stresses $\sigma_1+\sigma_2+\sigma_3$ (where: σ_1 – stress directed parallel to the specimen surface; σ_2 – stress in the same plain, but directed perpendicularly to σ_1; and σ_3 – stress directed normally to the specimen surface) normally directed stress σ_3 is equal zero. So, measured value σ consisted of two perpendicular stresses $\sigma_1+\sigma_2$, but specific value each of them cannot be estimated separately. Unfortunately, for specimens having another (not flat) shape X-ray method could not be applied. That is why we proposed some modification of usual approach based on following simplification: cylindrical specimens were cut longitudinally (Fig. 7a, b), and caused by this obvious changes of general stress condition were not taken onto account. Then an x-ray beam collimated to a width not exceeding 1 mm was positioned on a thin layer closest to the surface, moved incrementally to deeper layers (Fig.7b) through the specimen center and then to the opposite, outer-diameter surface. Full θ-2θ diffraction patterns were recorded at each location, and diffraction line broadening was estimated to evaluate increased density of crystallographic defects in material. For each location tilting of the specimen around the X-axis (Fig. 7c) was done enabling the determination of the peak shift of x-ray lines, that direction defines the sign (compressive versus tensile) of stresses formed during LRHT, whereas shift values - their magnitude. Based on the last data residual stresses were quantitatively evaluated using the following equation [5, 6]:

$$\sigma_1 + \sigma_2 = - (\Delta d / d_0) \, (E/\mu); \qquad\qquad (1)$$

where $\sigma_1 + \sigma_2$ – above mentioned sum of residual stress in plane of specimen section, d_0 – lattice parameter (interfacial distance) for non-stressed condition, Δd – difference in lattice parameter between stressed and non-stressed conditions, E and μ – respectively Young and Poisson modules.

Authors understood, that proposed method is not absolutely correct because don't take into account changes of stress fields resulted from specimen cutting. However, we consider such an approach as useful just for qualitative evaluation of stressed condition appeared on LRHT in cylindrical specimens.

According to the general viewpoints of X-Ray methods of residual stresses evaluation in metallic materials [5 - 7] micro-stresses, appeared mainly as a result of increased density of crystalline structure defects and localized within the least element of microstructure (in our case - α-grains), resulted in broadening of corresponding XRD peaks. The inputs of defects density and produced by its micro-stresses in peaks broadening cannot be divided. If micro-stresses couldn't relax within single microstructural feature, and/or their ensemble in some locations has common vector, they are resulting in formation of macro-stresses propagating trough much longer than for micro-stresses distances. Such kind of residual stresses appears in shifting of proper peaks which sign follows from equation (1), namely: left shift means appearance of tensile stresses, right shift – compressive stresses.

Results of the broadening of $(0002)_\alpha$ and $(101)_\alpha$ XRD peaks measurement are shown in Fig. 8. A closer examination of the line-broadening data for the LRHT trial lasting 2.8 s revealed two maxima near the surface – one at ~0.7 mm from the surface, and the second at a depth of ~1.5 mm (Figs. 8a, b). Between these two maxima, the broadening curve should go through a minimum equal to the level of broadening measured in the center of the specimen, because just at this position on specimen tilting direction of relevant peaks shifting was changed to opposite one (Fig.3) [5, 6].

However, such was not observed in that particular case, most likely because the x-ray beam obviously was too wide to resolve the local minimum between the two maxima. Taking into account the peaks shifting on tilting (Fig.9), it was concluded that the residual macro-stresses in the different layers had different signs. Specifically, in the layers closest to the surface (i.e., 0.3 mm from the surface), the alpha-phase peaks shifted to higher angles (Fig. 9a) thus providing evidence of compressive residual stresses [7, 8]. In deeper layers, that correspond to assumed local minimum in Fig.8, there was no difference in position of the x-ray lines for the tilted and untilted reflections (Fig. 9b) thus suggesting an absence of residual macro-stresses at this location. For the layer located ~1.1 mm from the surface, the reflections shifted again, but in this case to lower angles (Fig. 9c), indicating macro-stresses those were tensile in nature.
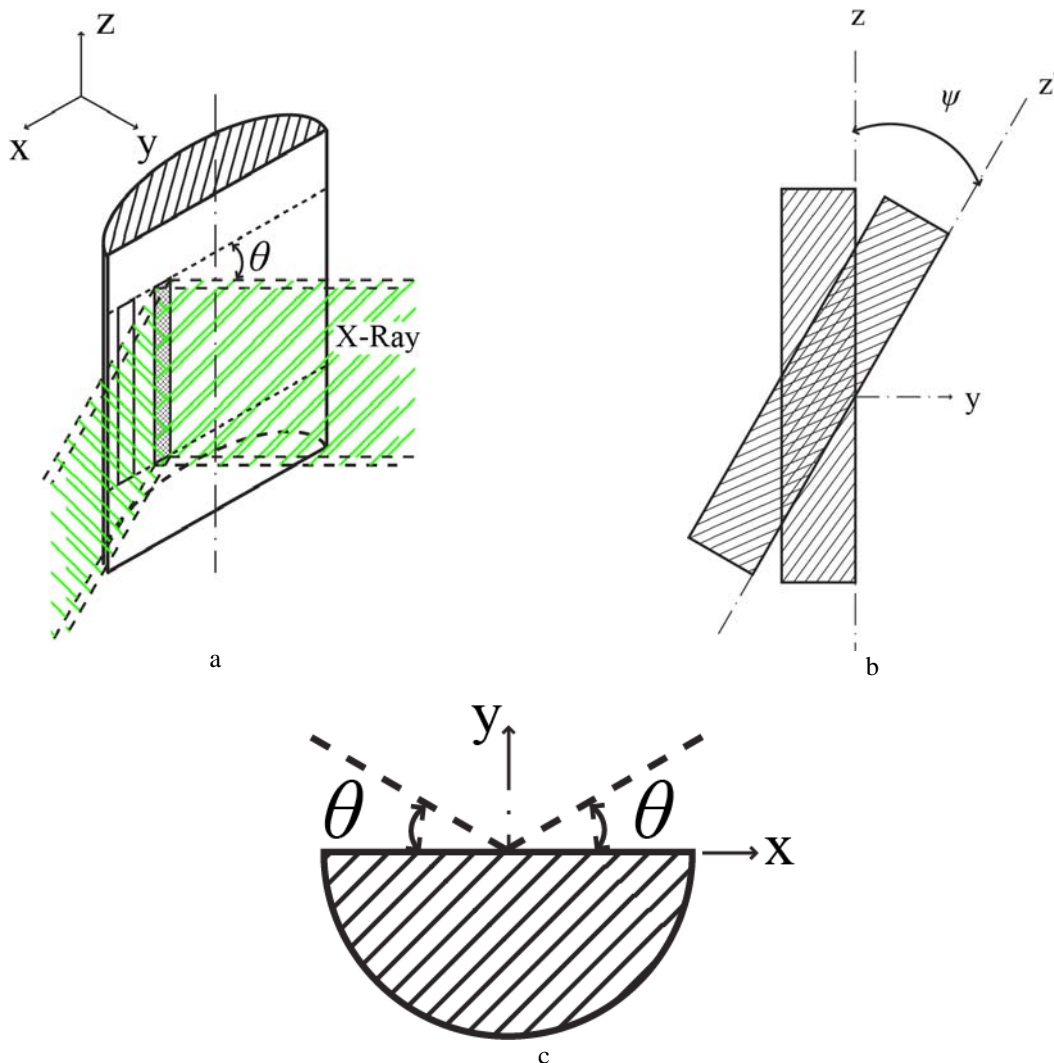
Fig. 7. Scheme of X-ray experiment for residual stresses evaluation; (a) – step-by-step X-ray irradiation of cut through the diameter specimen starting from position as close as possible to it's surface; (b) – specimen tilting relatively X-axis to estimate sign of internal stress; (c) – view from top of (a) illustrating common case of X-ray θ-2θ exposure.
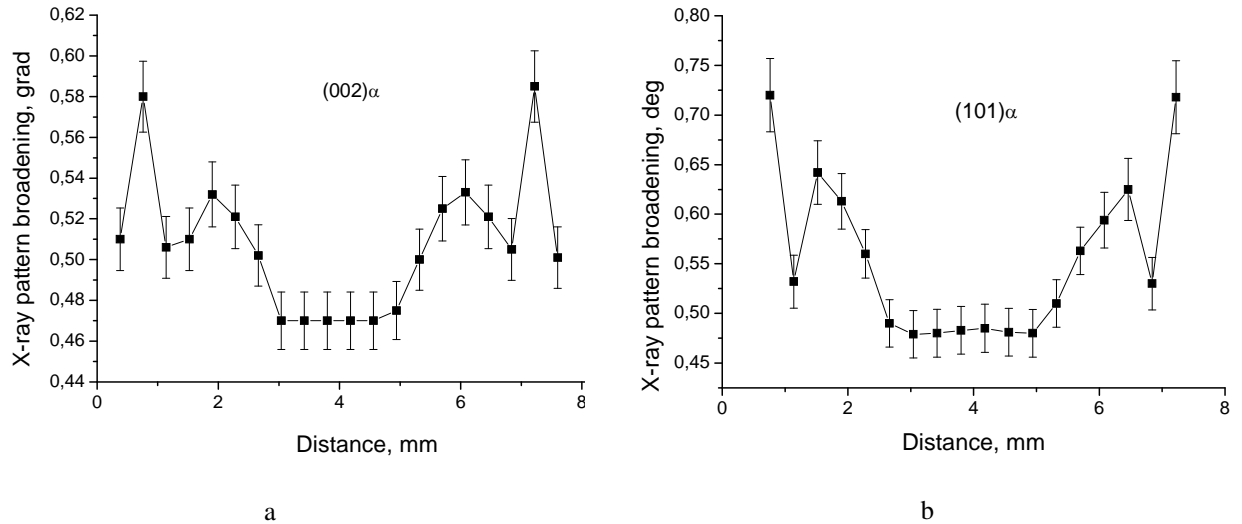
Fig. 8. X-ray pattern broadening of CP-Ti after LRHT (5 kWt, 2.8 s/WQ). (a) - for (002)α, (b) – for (101)α.
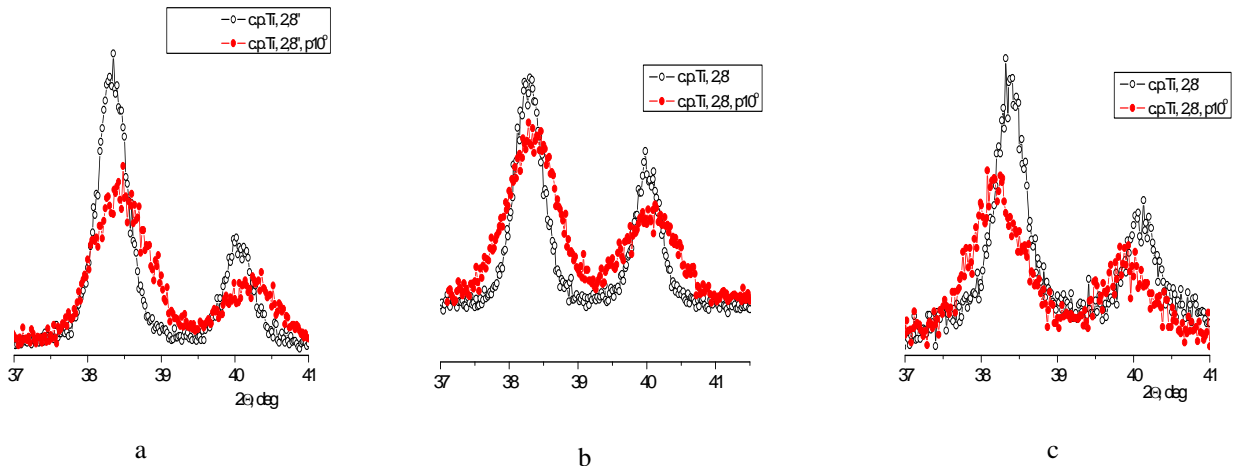
Fig. 9. ″Θ–2Θ″ X-ray patterns for the specimen after LRHT (5 kWt, 2.8″/WQ) recorded from (distance from the surface); (a) – of about 0.3 mm; (b) – of about 0.8 mm; (c) – of about 1.1 mm. Black (open) points – recorded in specimen position with zero tilting relatively Z-axis; Red (close) points – recorded in specimen position tilted by 10° angle relatively Z-axis.

An increase in the duration of LRHT from 2.8 s to 3.0 s changed both the character of the x-ray line-broadening distributions across the specimen (Figs. 8a versus 8c) and XRD peaks shifting. The last one was quantified in more detail using Equation (1) to estimate the corresponding residual stresses (Fig. 10). For the trial using a duration of 2.8 s (Fig. 4a), the near-surface layer exhibited a high compressive stress, the mid-radius had a tensile stress, and the core (r ≤ 2 mm) has essentially no residual stress (Fig. 10a). For the second case (heating time of 3 s), the residual-stress distribution was different. The surface layer ~2-mm thick was characterized by compressive stresses, whereas the entire central part of the specimen had tensile residual stresses (Fig. 10b).

It should be born in mind that the measured residual stresses should be viewed qualitatively because of the sectioning method used to expose the cross-section. Nevertheless, the technique does qualitatively illustrate the important effect of heating time during LRHT on residual-stress evolution.

<p align="center">a   b</p>
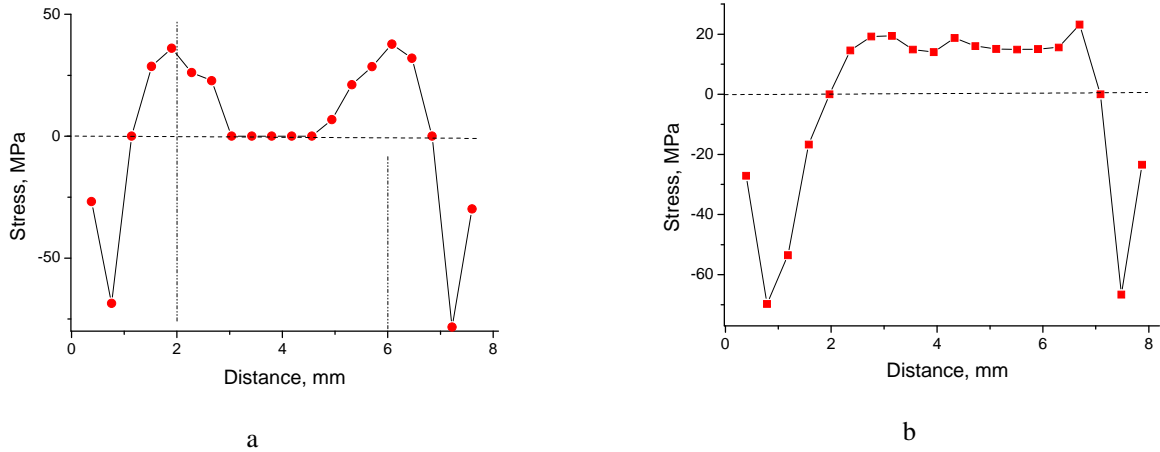
Fig. 10. The residual stresses distribution as a function of radial location in LHRT specimens heat treated (and then water quenched) using 5 kW power for (a) 2.8 s or (b) 3 s.

3.3. Measurement of thermal fields, formed in specimens during LRHT.

During project performing appeared a necessity to obtain information about real temperature distribution developed during induction LRHT of the cylindrical specimens was estimated using an approximate approach. Specifically, the temperature at the surface was measured using a two-color pyrometer (IMPAC IGA100) having a 0.2 µs response time. The skin/penetration depth (1.2 mm) was estimated using standard formulas and an average resistivity for temperatures between room temperature and 1000°C [1, 3]. As a first approximation, it was assumed that the temperature within the penetration depth was constant and equal to the measured surface temperature. The approximate temperature distribution $T(r, t)$ between the skin layer and the center of specimen as a function of radial position r and time t was then estimated using taken from [9] relation for the heating of a cylinder of infinite length:

$$T(r,t) - T_0 \approx k \left[A \frac{t}{R^2} - B \left(1 - 2 \frac{r^2}{R^2} \right) \right]; \qquad (2)$$

where: T_0 is an initial temperature of material; R is the outer radius of the cylinder.
Constants k, A and B are equal:
      $k = qR/\lambda$; $A = 2a$; $B = 0.25$; and $a = \lambda/c\rho$
where: q – heat flow; λ – heat conductivity; c – heat capacity; ρ – density of CP-Ti.

Solution of equation (2) is based on a boundary condition comprising constant heat flow from the surface of the cylinder (i.e., from skin-layer). Symbol "≈" in (2) is correct for times $0 < t < 0.6R^2/a$, and for all times $t \geq 0.6R^2/a$ (for our case this is 1.12 sec) it should be replaced by symbol "=".

Obtained temperature profiles based on the measured surface temperatures and the analysis briefly summarized above are shown in Fig. 11 for three studied alloys and different heating times. In all cases, the difference between the maximum temperature (at the surface) and the minimum temperature (at the center of the specimen) was the same. The measured for CP-Ti location of the boundary between the transformed and untransformed regions (e.g., the boundary between the dark- and light- etching regions in Figure 3) is also plotted in Figure 11a as individual data points. All of these measurements lay close to horizontal line indicating that the postulated value of T_β (960°C) corresponding to rapid heating conditions for CP-Ti was reasonable. Thus, it can be concluded that the overall method for quantifying the radial temperature distribution was plausible.
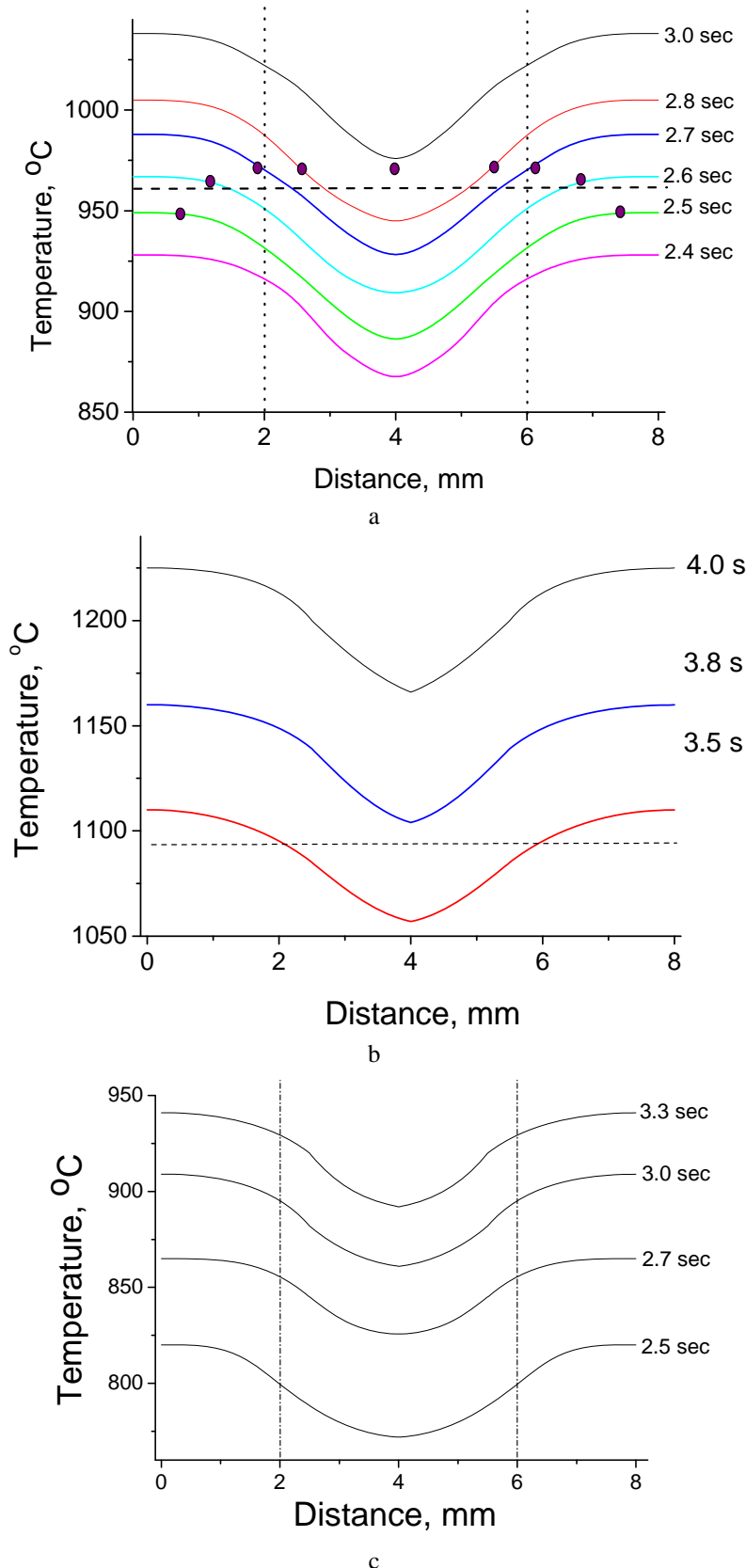
Fig. 11. Calculated radial temperature distribution across an 8-mm diameter specimen as a function of LRHT heating time using a 5kW (a) and 4 kWt power supply; (a) CP-Ti, (b) Ti-6-4, and (c) TIMETAL-LCB. (a) - the horizontal dashed line corresponds to T_β for CP-Ti under rapid-heating conditions. The vertical dotted lines corespond to the gage diameter of post-heat-treatment tension specimens. (a) – the points indicate the visible boundary between regions heated above and below T_β.

4. RESULTS AND DISCUSSIONS

4.1. CP-. Titanium

First of all it is necessary to underline, that in this study CP-Ti was taken as an important reference (basic) material with which other materials will be compared in subsequent investigations.

Typical examples of LRHT-treated CP-Ti macrostructure are shown in Fig. 3, where difference between zones heated above and below beta transus temperature T_β is clear seen as difference in surface etching. Such a difference suggests that this possibly is a result of formation of titanium martensite on quenching, but used LM magnifications did not allow us to identify it. Taking into account dependence of $\alpha \rightarrow \beta \rightarrow \alpha$ transformed fraction on the time of treatment (Fig. 5) and keeping in mind that gage diameters of tensile and fatigue specimens were 4 and 3.8 mm respectively, for further investigations we chose treatments with following durations: 2.6, 2.8 and 3.0 seconds. These correspond to 70, 83 and 100% volume fraction of material heated above T_β temperature in Ø 8 mm specimen.

Fig. 12 represents an example of microhardness distribution in cross-section of LRHT-treated specimen after 5 kWt, 2.8 sec. It is possible to mark out three specific zones: (1) – where microhardness level is a little lower than the average one, (2) – where it is higher, than the average one, and (3) – which corresponds to initial average level. In this case the boundary between heated above and below T_β layers is in the zone with higher level of microhardness. Investigation of microstructure in each zone showed that in the first one microstructure with increased average size of alpha-grains was formed as a result of heating to high temperatures (Fig. 13a, b), and coarser grains correspond to outer layers, where temperature was higher. Also it is possible to mention about visible amount of twins formed in this zone. At the boundary between the zones heated above and below T_β temperature only initial stages of alpha-grain growth were seen (Fig. 13c), while in the specimen core (where temperature was essentially lower than T_β), microstructure was similar to initial (annealed) one (Fig. 13d). Microstructure of other specimens LRHT-treated during different times differs from above mentioned only by position of boundary between zones heated above and below T_β. For example, for treatment during 2.8 sec microstructure in the specimen center was similar to one presented in Fig. 13c; for treatment during 3.0 sec microstructure in the specimen center was similar to one shown in Fig. 13b. Formation of coarser alpha-grains in the zone heated above T_β temperature may cause in observed some decrease of microhardness, but microhardness increase in zone (2) can not be explained by its microstructure. Taking into account conditions of heating and cooling, namely their rates which were close to $400^{\circ}C/s$, it is rather naturally to assume that increase in microhardness can be a result of formation of high internal stresses, which in turn may cause in local plastic deformation and increase in defects density. In other words, during the whole cycle of fast heating and cooling (quenching) specimens have twice undergone specific "thermal shock", when during only 4 – 5 seconds they were heated up to high temperature and right away cooled to room temperature.

Basing on above data we chose for tensile testing following structural conditions of this material: (1) - initial (annealed), (2 – 4) – LRHT- treated with different durations, having in mind to obtain different volume fractions of layer heated above T_β (for 4 mm gage diameter of specimens). Also one additional condition (5) – finally aged ($500^{\circ}C$, 2 h) was prepared and tested to clarify the role of internal stresses. Relevant results of tensile tests for all conditions are listed in Table 1. Typical examples of technical stress-strain curves are shown in Fig.14.

Analysis of presented in Table data allows to conclude that increase in LRHT-treated above T_β volume fraction of CP-Ti caused in monotonic growth of strength (for instance, UTS increased from 482 MPa in initial condition to 522 for 100% heated above T_β material), but at the same time total elongation dramatically decreased (in two times), while reduction of area was approximately the same. Comparison of fracture surfaces of all conditions did not reveal any principal difference

(Fig.15)[1]; it is possible just to mention about more shallow dimples in LRHT condition, that is related with discussed above lower plasticity of this condition. Application of final aging for 100% heated above T_β material led to rather complete renewal of properties of initial condition (compare pp. 1 and 5 in Table 1); only yield strength became a little lower, obviously, due to a bigger average size of alpha-grains. In general these tensile results showed, that LRHT- treatment allows to vary in some ranges strength and ductility of CP-Ti probably due to formation of some thermal stresses and/or some deformation defects. But monotonic growth of yield stress with increase of treatment duration could not be related with internal stresses and, possibly, may be attributed to formation of martensite substructure inside coarse alpha-grains.

On the base of analysis of above data two kinds of specimens, which had the highest difference in tensile properties, were chosen for fatigue testing: (1) initial annealed condition and (2) LRHT-treated 5 kWt, 3.0 sec condition. Results of fatigue tests are presented in Fig. 16. It is seen, that initial condition was characterized by rather common as for this material curve with fatigue limit of 250 MPa. At the same time curve for specimens after LRHT was characterized by increased in 1.5 times endurance limit and very flat curve in the high- cycle region. The last fact says about some instability of LRHT-treated material. However, likewise tensile specimens, fatigue fracture surfaces have very similar appearance (Fig. 17) – in both cases cracks were initiated on the surface and propagated in the same way. Only at higher stress amplitude several cracks nucleation sites were observed (Fig.17e). Nevertheless, obtained improvement of fatigue properties looks very attractive and in absolute increase exceeds even results obtained after special surface mechanical hardening [10].

In general, the fact of visible increase of mechanical properties of CP-Ti after LRHT looks rather attractive since, as it is well known, this material could not be strengthened via conventional thermal hardening approaches because absence of alloying elements and, therefore, not formed and not decomposed metastable phases.
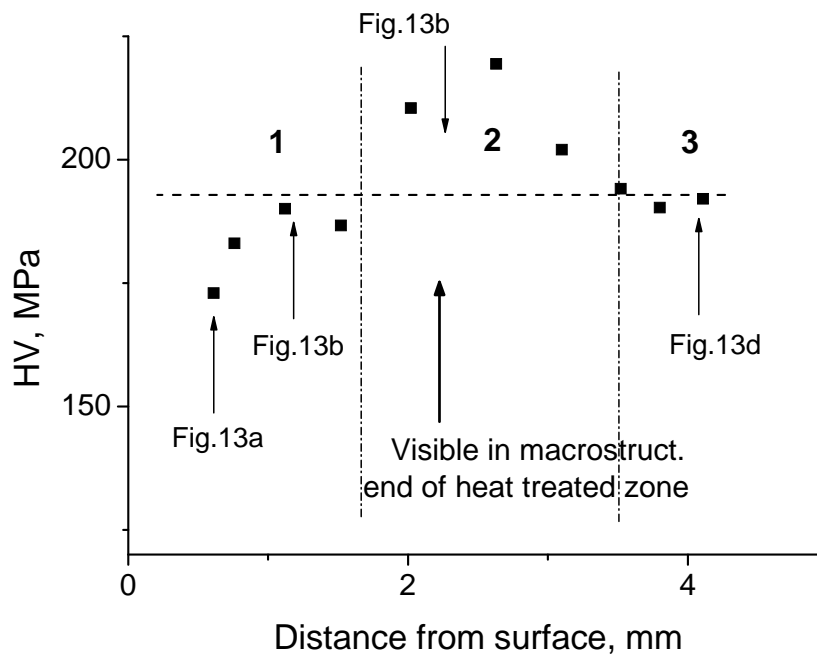
Fig.12. Microhardness vs. distance from the surface for CP-Ti after LRHT (5 kWt, 2.6 sec). Dashed line corresponds to average level of microhardness of initial annealed specimen.

---

[1] some asymmetry of transverse deformation of specimens during neck formation (Fig. 9a and c)may be explained by specific crystallographic texture of initial rod.
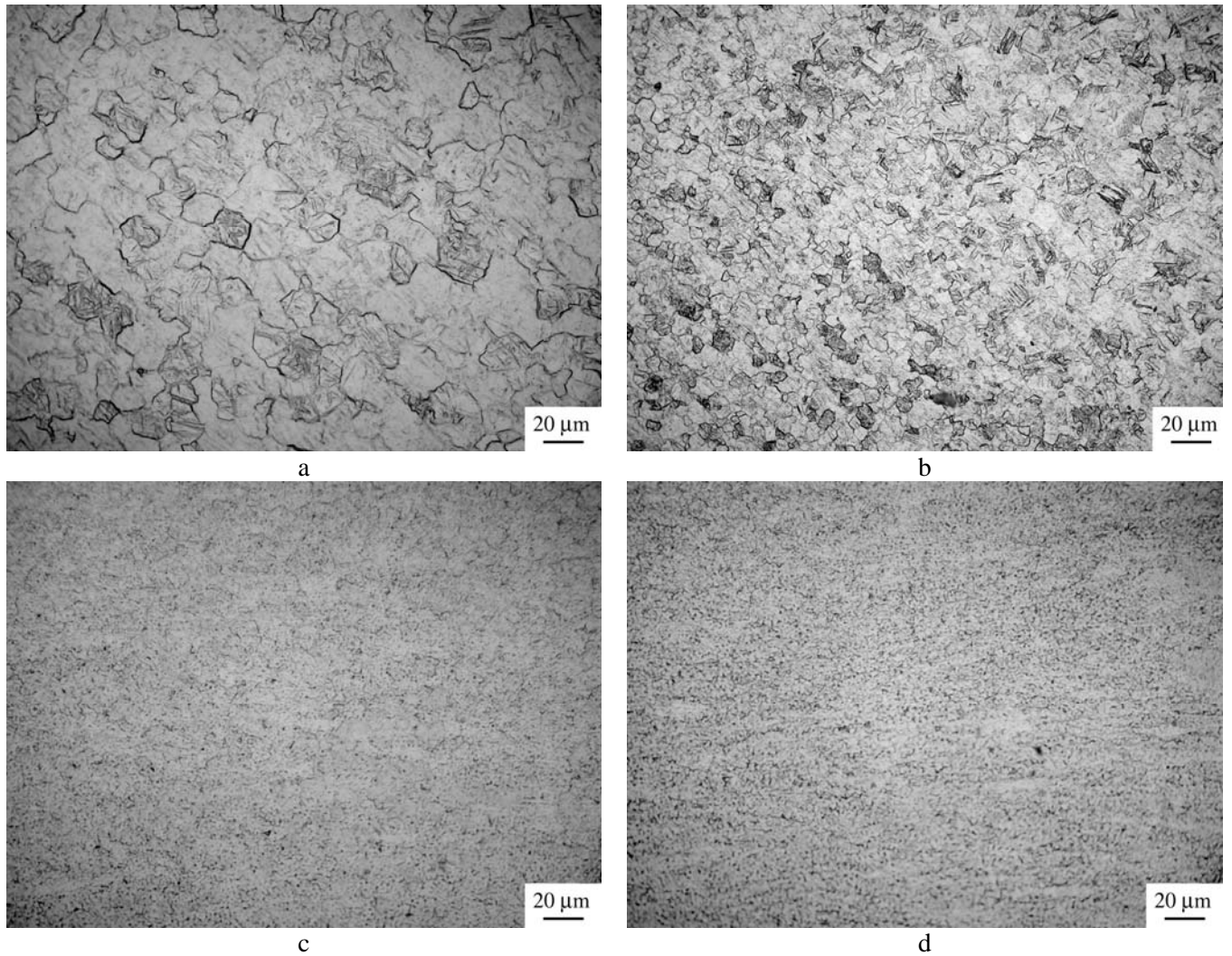
Fig.13. Typical microstructure of CP-Ti in: (a, b) surface (heated above T_β), (c) transition and (d) core (where temperature was below T_β) zones. All locations are shown by arrows in Fig.6 above. LM

Table 1
Mechanical Properties of CP-Ti in different conditions

##	Condition	Volume fraction heated above T_β, %*	Tensile properties			
			YS, MPa	UTS, MPa	El, %	RA, %
1	Initial, annealed 800°C, 0.5 h	0	366	482	30.9	57.4
2	+ LHRT: 5 kWt, 2.6″/WQ	~15	429	518	23.4	67.1
3	+ LHRT: 5 kWt, 2.8″/WQ	~40	402	503	15.7	61.9
4	+ LHRT: 5 kWt, 3.0″/WQ	100	413	522	13.2	55.1
5	+ LHRT: 5 kWt, 3.0″/WQ + 500°C, 2h	100	347	484	31.1	57.9

* Gage Ø 4 mm was taken into calculation.

Specimen 1 to 3
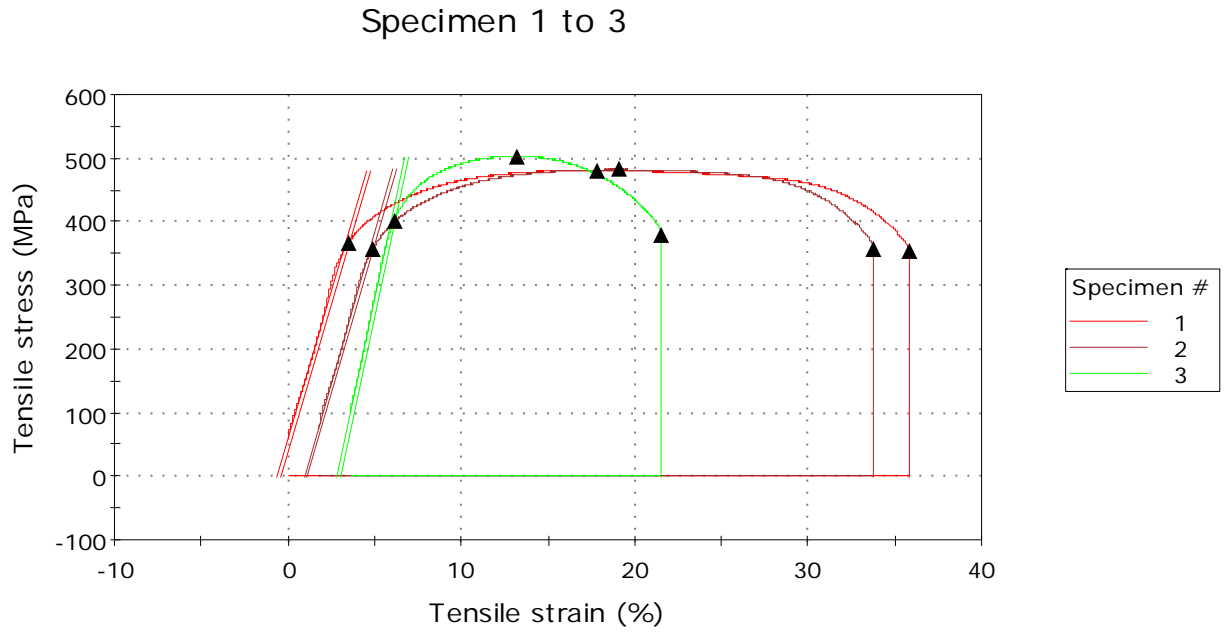
Fig.14. Typical example of technical tensile curves comparing CP-Ti specimens in: (1 & 2) initial (annealed) and (3) surface heated 5 kWt, 2.8″ conditions.
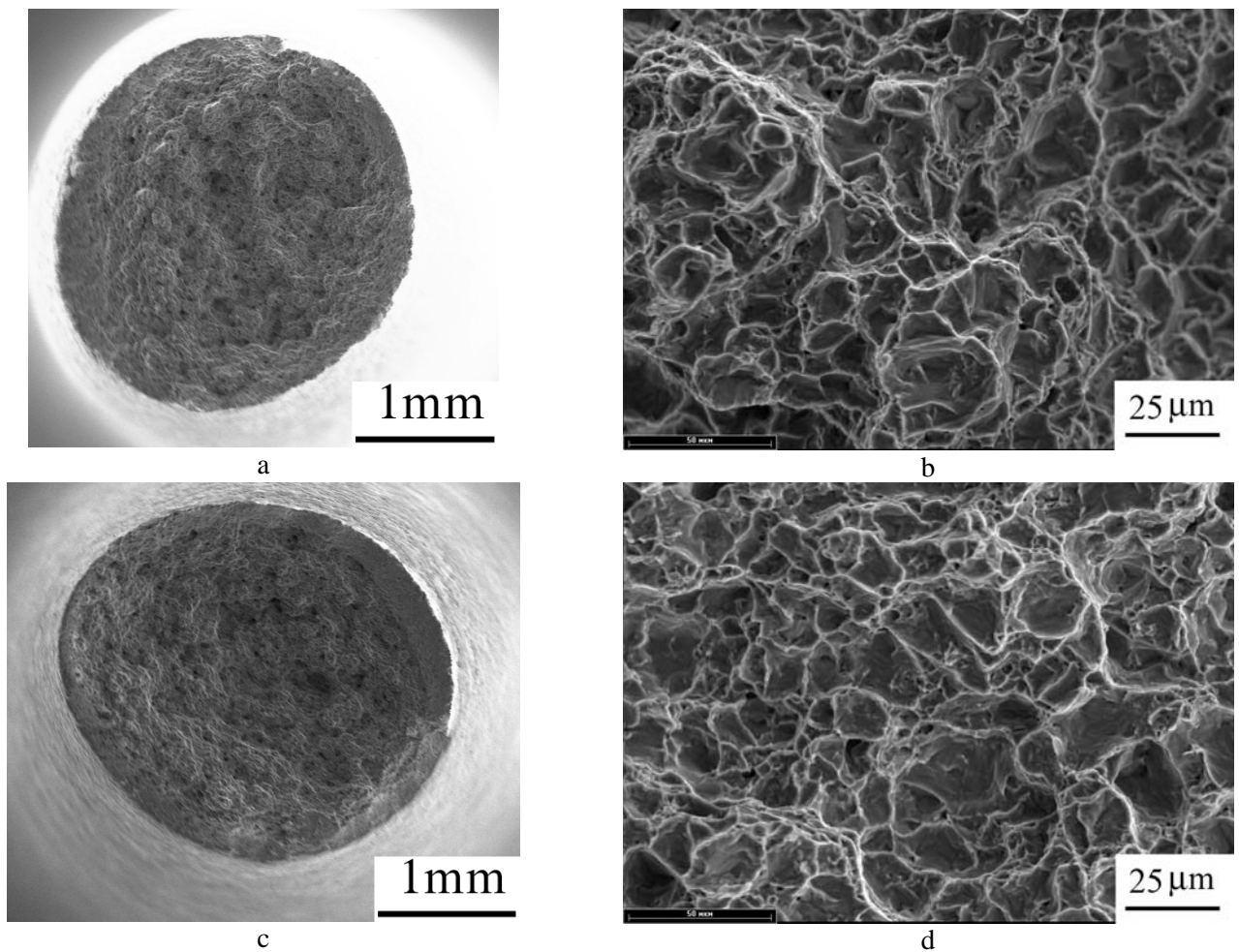
Fig.15. Typical fracture surfaces of CP-Ti tensile specimens in (a, b) initial and (c, d) LRHT (5 kWt, 3.0″) conditions. SEM.
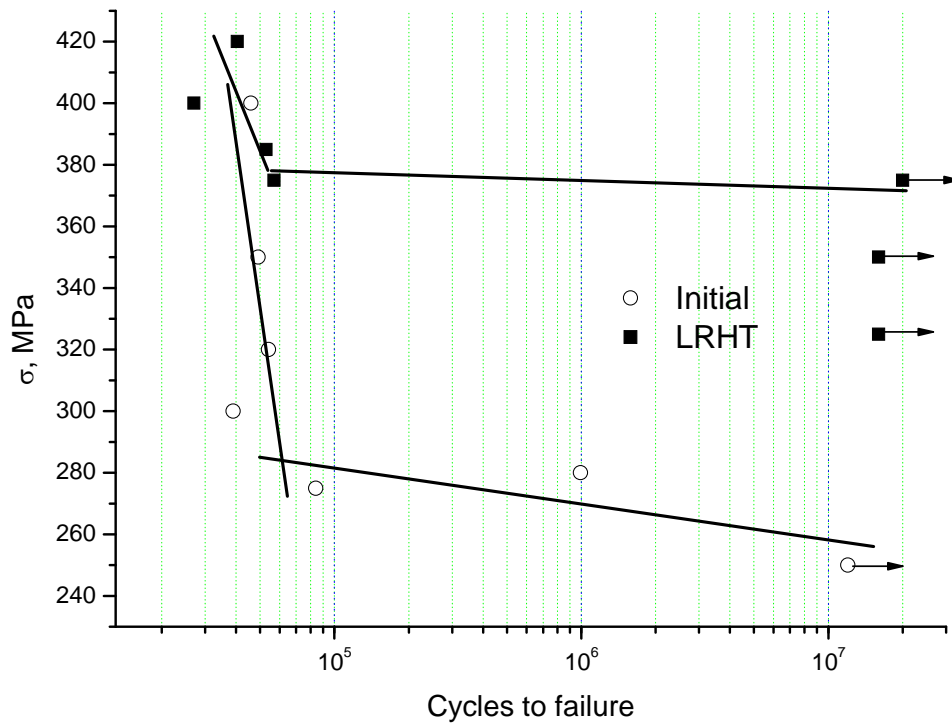
Fig.16. Fatigue data for CP-Ti in the initial (annealed) and LRHT (5 kWt, 3.0 sec) conditions.

e
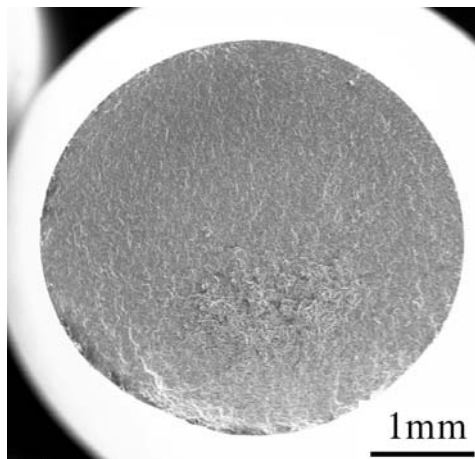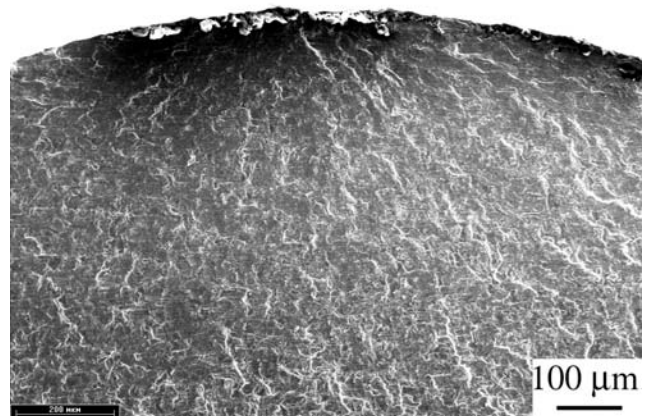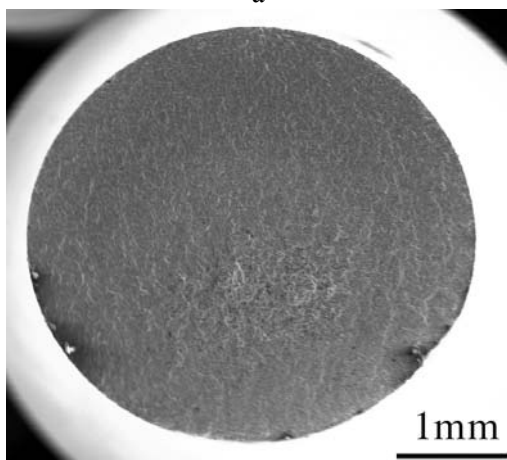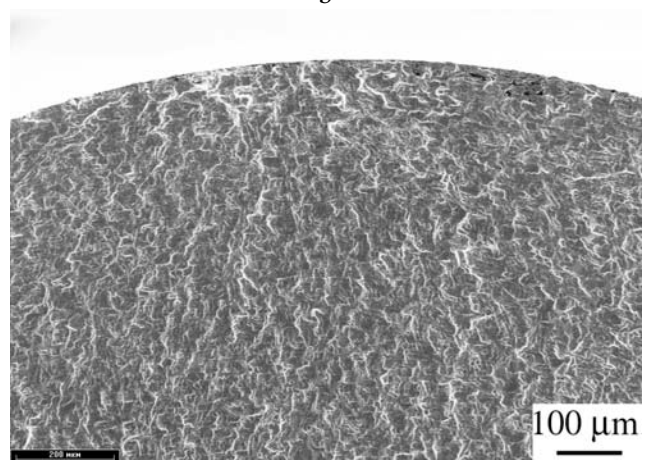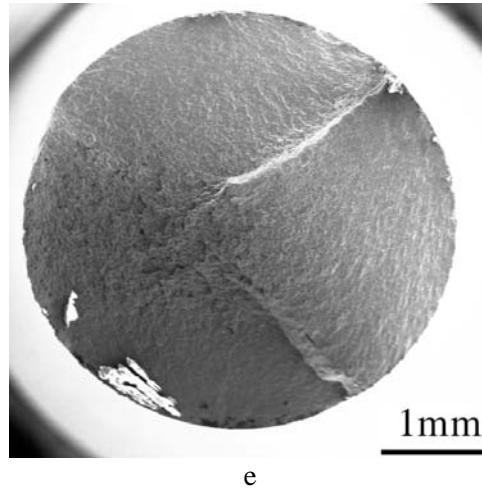
Fig. 17. Typical fracture surfaces of CP-Ti fatigue specimens in (a, b) initial and (c - e) LRHT (5 kWt, 3.0″) conditions. SEM. (a, b) tested at 280 MPa, (c, d) tested at 375 MPa, (e) tested at 420 MPa.

So, application of LRHT comprising heating rates to 400°C/s and final water quenching, radial gradients in alpha-grain size, substructure/martensite, and residual stress are developed. This leads to improvements in strength and fatigue behavior with little-to-no effect on RA; only the tensile ductility is deleteriously affected. The principal strengthening mechanism associated with LRHT of CP-Ti was concluded to be the formation of substructure and martensite during rapid heating and cooling.

4.2. Ti-6Al-4V (Ti-6-4) alloy

4.2.1. Initial equiaxed (globular) microstructure

For this alloy after preliminary tests it was considered reasonable to employ LRHT with 4 kWt applied power as one allowing to form more smooth and uniform shape of thermal front. This value of applied power ensured heating above corresponding T_β of 100% in Ø 8 mm specimens after 4 sec, while 3.8 sec LRHT caused in approximately 45% transformed material of specimen with gage Ø 4 mm.

Microstructures of different layers in Ti-6-4 specimens after LRHT during 3.8 sec and 4.0 sec are shown in Figs. 18 and 19 respectively. In the first case just after LRHT no evidences of heating above T_β (in this alloy they should be in the form of so called beta-transformed microstructure [11]) were observed (Fig.18a, b), obviously, because of too fine martensite formed on quenching. Additional annealing (900°C, 1h) was performed to reveal grain structure – at this temperature alpha phase precipitates predominantly on grain boundaries [12]. And really, after such annealing rather coarse grain boundary alpha was found as decorating beta-grains boundary (Fig. 18d, f); beta-grain size in upper beta-transformed layer was estimated as close to 20 μm; in deeper zone beta-grains were not larger than 10 μm, while in the center of the specimen microstructure remained equiaxed with some increase in average size (or formation of microstructure of bi-modal type because of exposure at 900°C). Longer LRHT (4.0 sec) resulted in coarser beta-grains: average grain size in surface layer was of about 35 μm (Fig.19a - d), deeper layers were characterized by 20 μm grain size (Fig. 19e), and in the specimen center average grain size was of about 10 μm (Fig. 19f).

Ti-6-4 material subjected to these two LRHT regimes was tensile tested in as-quenched as well as in subsequently aged conditions, and obtained results were compared with initial (annealed 800°C, 1h) condition (Table 2).

Presented in Table 2 data illustrates essential increase in strength characteristics of Ti-6-4 material after LRHT itself as well as with subsequent aging. It is interesting to note that as-quenched after LRHT conditions (pp. 2 and 4 in Table 2; typical examples of technical stress-strain

curves are presented in Fig. 20) were characterized by some increase in strength and most pronounced drop of ductility, that may be associated with formation of hard but having limited plasticity martensitic phases, whereas phase-stable α+β conditions after LRHT + aging had better balance of strength and ductility. Difference between LRHT-treated for 3.8 sec and 4.0 sec specimens, i.e. between having 45% and 100% of beta-transformed volume fraction alloys, consisted in a higher strength and lower ductility in the last case due to a bigger part of strengthened material. Taking into account earlier obtained for the same alloy results [13, 14] showed that bulk RHT of this alloy allows to form fine-grained (with average grain size below 40 μm) with fine beta-transformed intragrain α+β microstructure ensuring ultimate tensile strength level not less than 1300 MPa with acceptable ductility. Our results look very close to those, but in our case presence of layers which differ in phase content and microstructural features, obviously, led to a non-uniform plastic deformation and comparatively early fracture, caused by weaker structural zone. At the same time obtained for 100% LRHT + aging balance of tensile strength and ductility looks rather attractive as for low-alloyed α+β alloy (p. 5 in Table 2).

Fracture surfaces of these specimens in different conditions are presented in Fig. 21. In initial equiaxed condition fracture was characterized with rather typical ductile dimples (Fig. 21b), while after LRHT and aging fracture surface had two separate zones – rim and central ones (Figs. 21c and f), where character of fracture was completely different. Close to surface zones contain traces of secondary cracking after both treatments (Figs. 21d and g), while in the central zones for the first case (3.8 sec) ductile dimples were found (Fig.21e) that is typical for initial equiaxed microstructure (compare with Fig.21b), and in the second case (4.0 sec) secondary cracking along grain boundaries of relatively fine beta-grains was clearly seen Fig.21i).

Observed peculiarities of tensile fracture of Ti6-4 material after LRHT can be rationalized in the following way. During uniaxial tension outer and inner layers of a specimen undergo equal elongation. At the same time, outer layers have higher strength and lower ductility as compared to inner ones. So, various fracture modes can occur. If difference in strength between outer and inner layers is quite higher, stresses developed between them during tension can result in cracks formation in the transition zone (delamination). If this does not occur, fracture can be initiated either in outer and in inner layers, depending on the relation between their ductility levels (Fig.22a, b). If ductility of inner layers is much higher, outer layers fail at first (Fig.22a). However, if total plastic elongations before fracture do not much differ for inner and outer layers, failure can be initiated in inner layers (Fig.22b). In our case it looks that fracture of tensile specimens after LRHT was initiated in transition zone (i.e. the first variant), then propagated to softer inner layers, and finished in outer layers (Fig.20c - i).
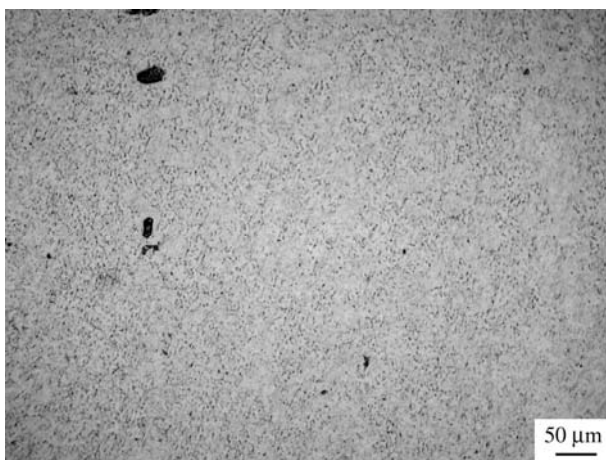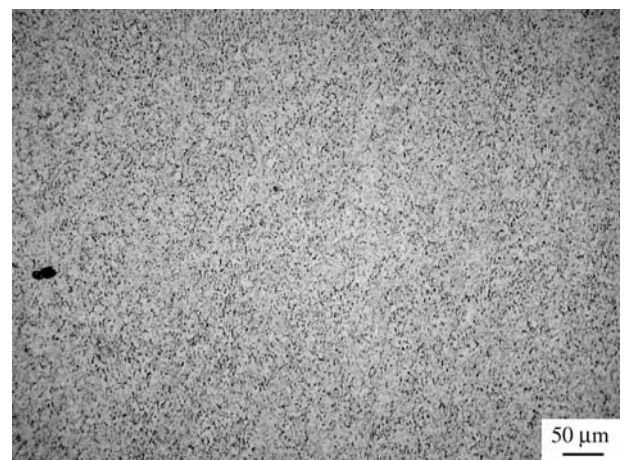
a   b
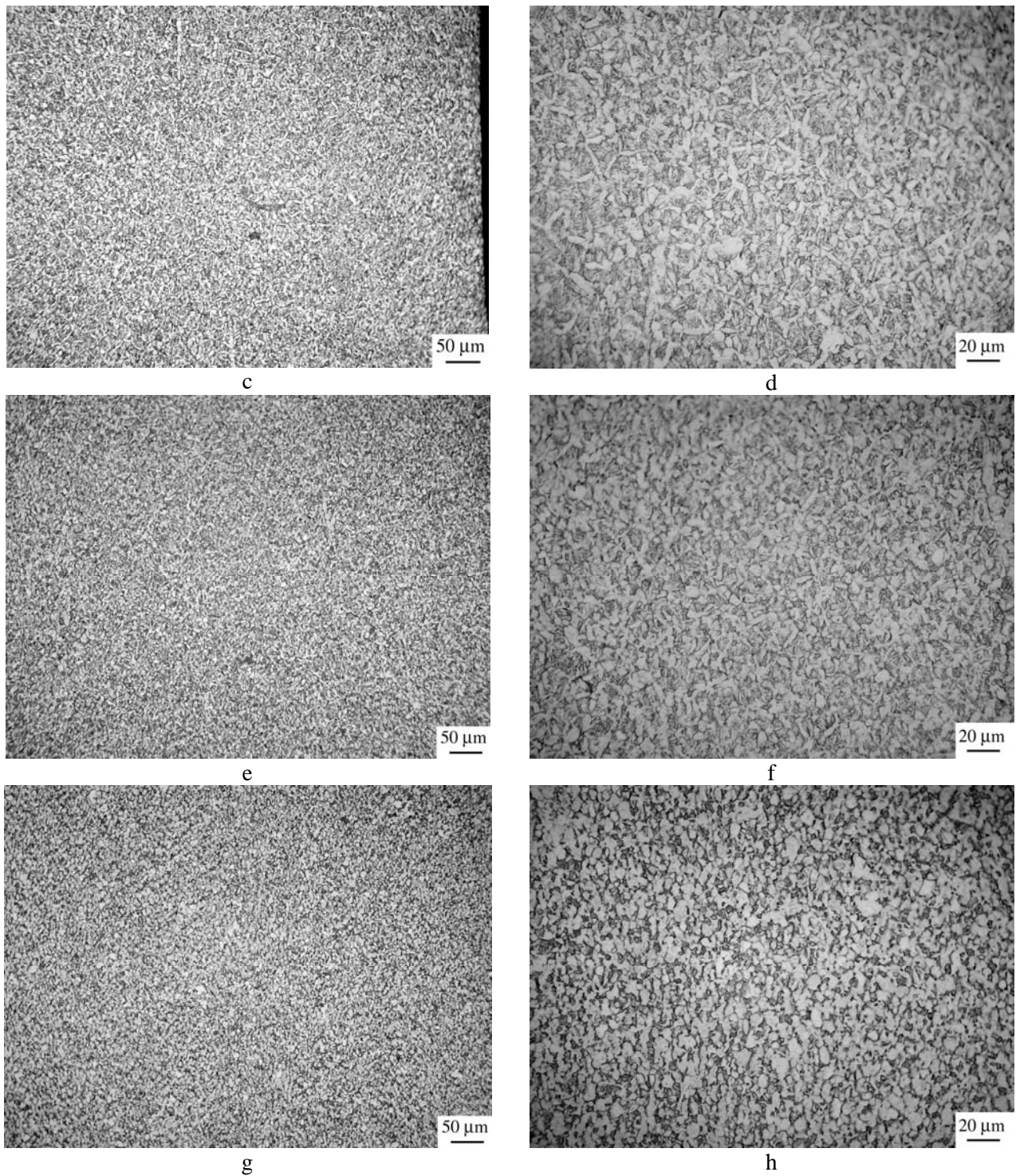
Fig.18. Microstructure of Ti-6-4 alloy after LRHT, 4 kWt, 3.8 sec. a, b – in quenched condition, c – h – the same + annealing in vacuum 900°C, 1h, cooling with furnace; a, c, d – LRHT-treated layer (specimen edge); b, e, f – transition zone; g, h – core of specimen.
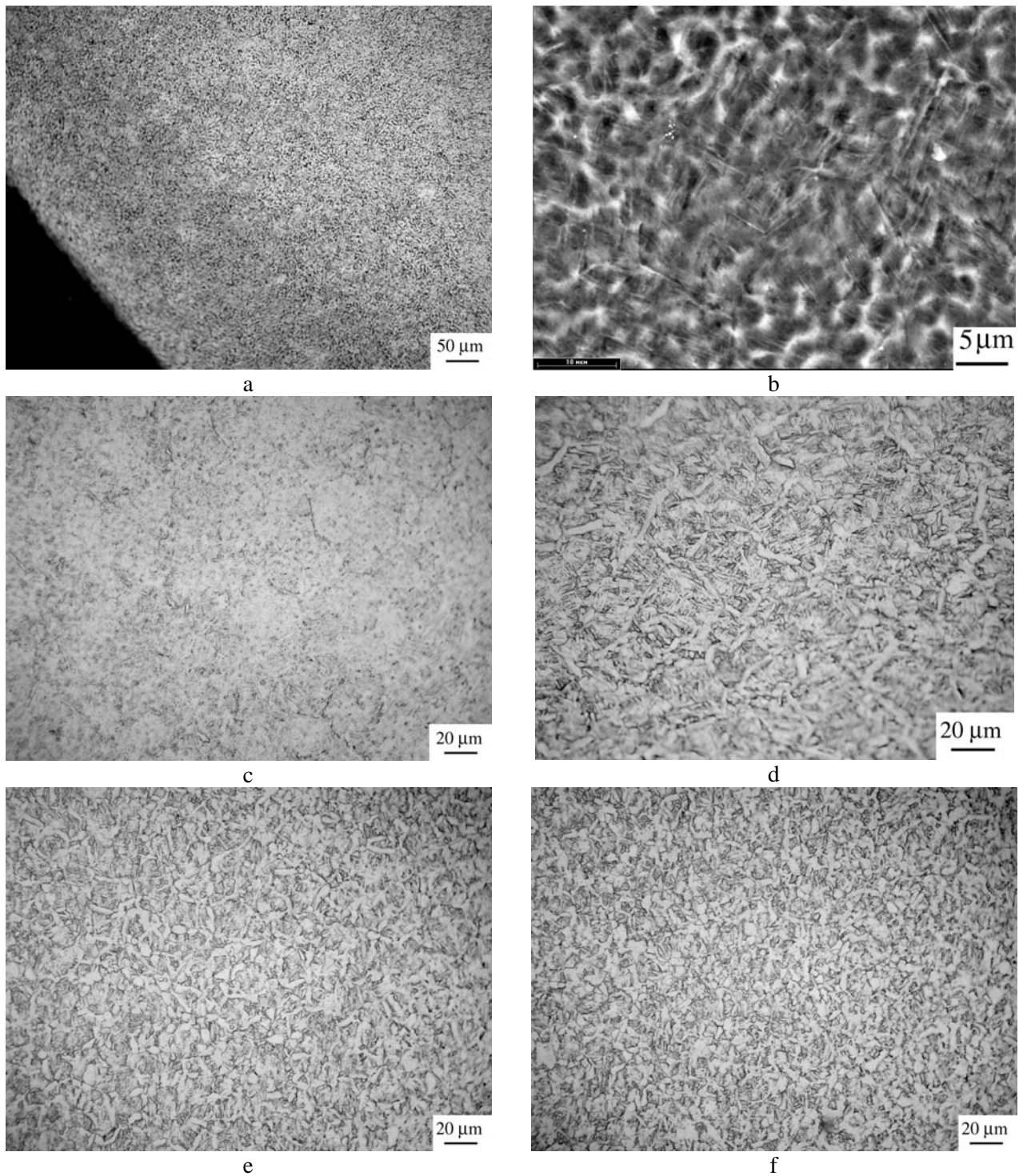
Fig. 19. Microstructure of Ti-6-4 alloy after LRHT, 4 kWt, 3.8 sec. a, b – quenched condition, c - +aging 550°C, 8h; d - +800°C, 1h, cooling with furnace; e, f - +900°C, 1h, cooling with furnace. a – d – specimen edge; e – transition zone, f – specimen center. a, c-f – LM; b – SEM.

Table 2
Mechanical Properties of Ti-6-4 in different conditions

##	Condition	Volume fraction heated above T_β, %*	Tensile properties			
			YS, MPa	UTS, MPa	El, %	RA, %
1	Initial, annealed 800°C, 1h	0	921	992	16.2	33.9
2	+ LRHT: 4kWt, 3.8 sec/WQ	~45	994	1062	6.81	35.2
3	+ LRHT: 4kWt, 3.8 sec/WQ +550°C, 6h	~45	1240	1254	7.69	49.9
4	+ LRHT: 4kWt, 4 sec/WQ	100	1180	1193	4,81	35,20
5	+ LRHT: 4kWt, 4 sec/WQ +550°C, 6h	100	1247	1285	5,75	36,87

* Gage Ø 4 mm was taken into consideration.
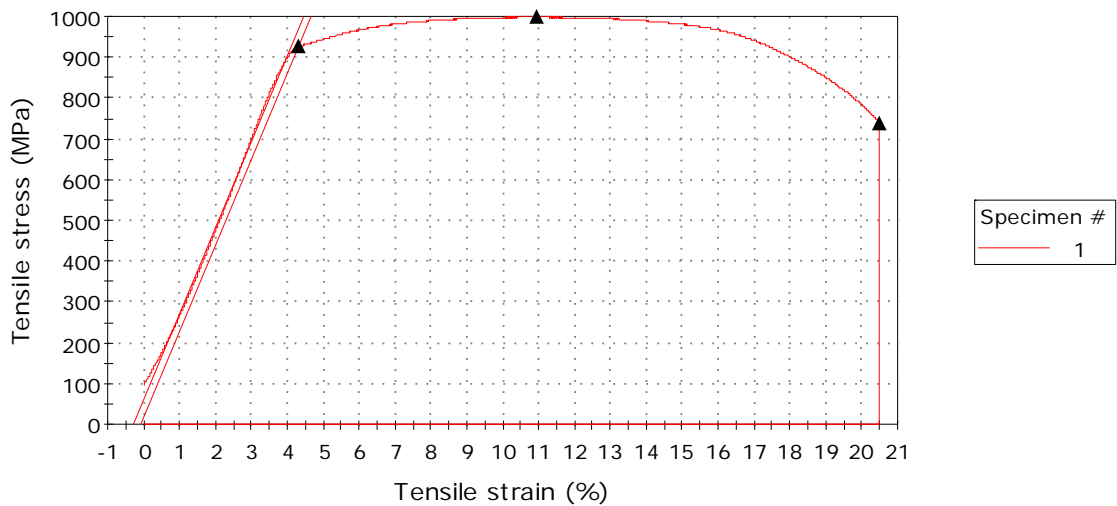
a
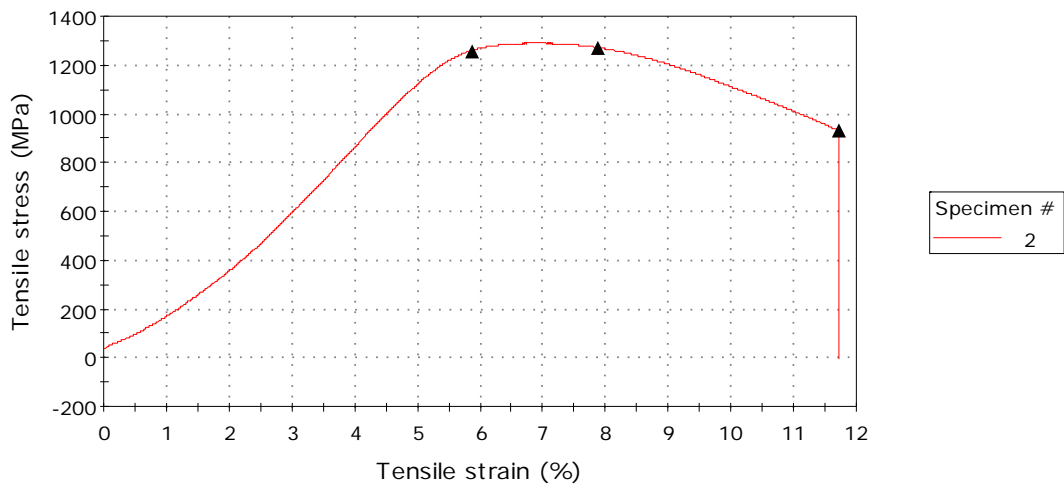
b

Fig. 20. Examples of technical stress-strain curves for Ti-6-4 in conditions: (a) – initial annealed, (b) – after LRHT (4kWt/3.8 sec/WQ+550°C, 6h).

a

b

c

d

e

f   g

i
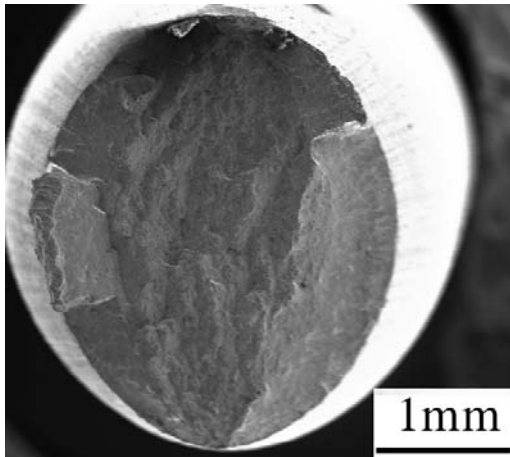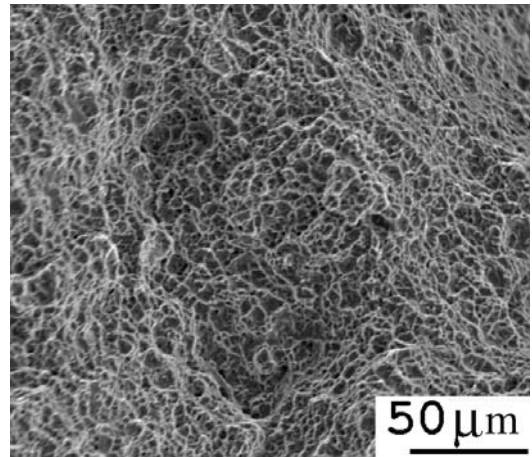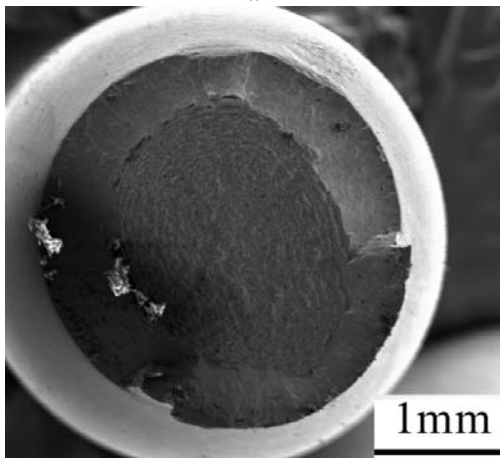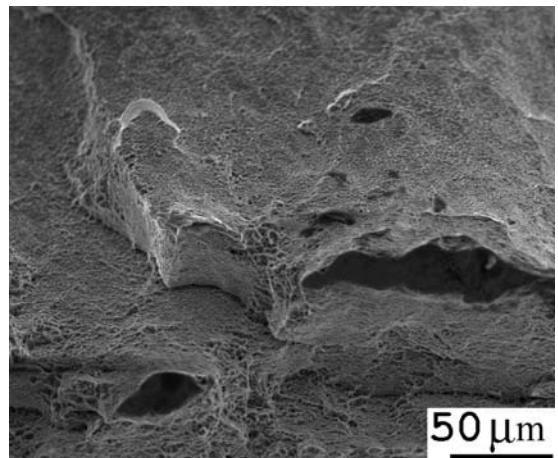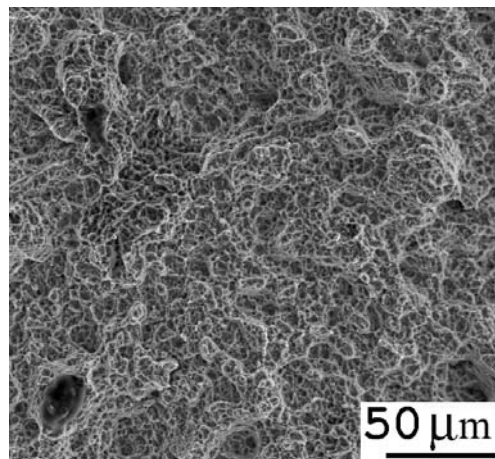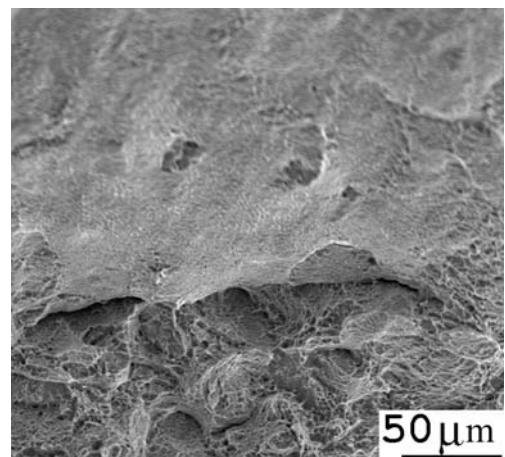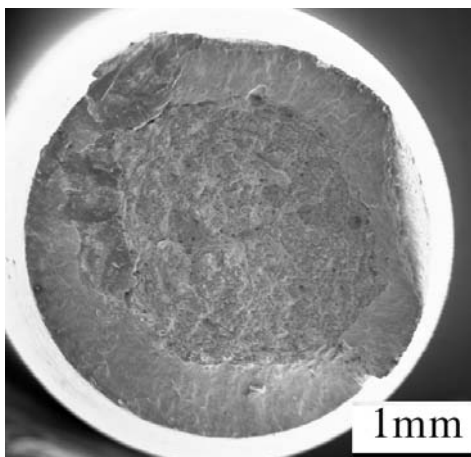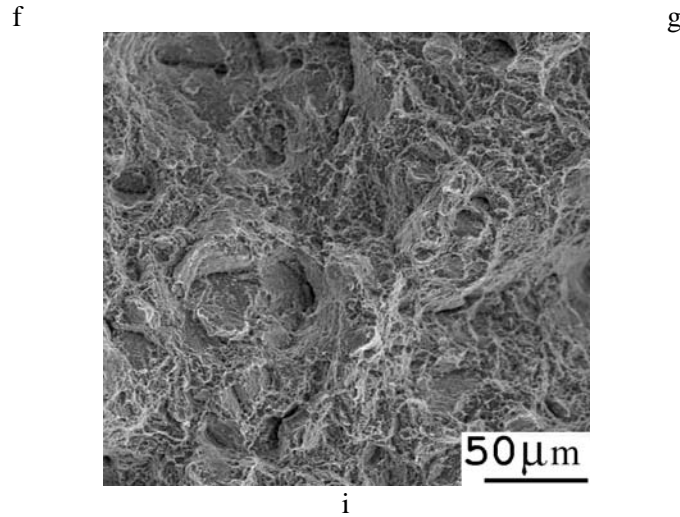
Fig.21. Fracture surfaces of Ti-6-4 in: (a, b) – initial equiaxed condition; (c – e) LRHT with 4 kWt, 3.8 sec + 550°C, 6h; (f – i) LRHT with 4 kWt, 4.0 sec + 550°C, 6h; (d, g) – surface zone; (e, i) – specimens' centre.
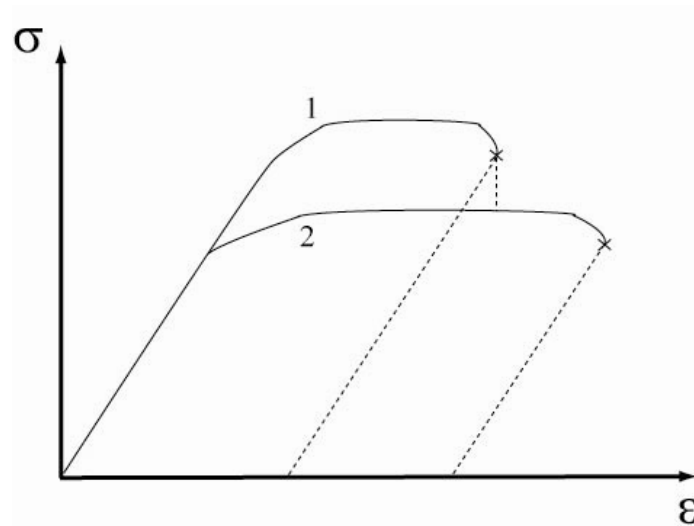
a
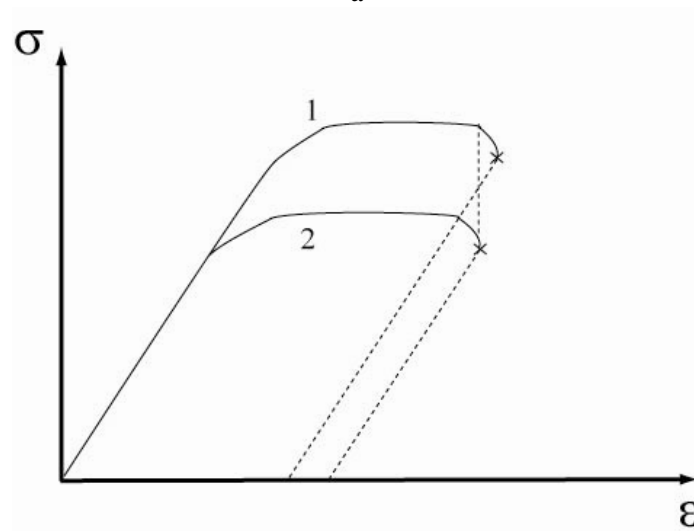
b

Fig. 22. Schematic presentation of tensile deformation curves for different layers in specimen with gradual microstructure; 1 – outer (LRHT-hardened) layers; 2 –core (not-hardened) zone. a – fracture was initiated in outer layers; b – fracture was initiated in inner layers.

a

b

c

d
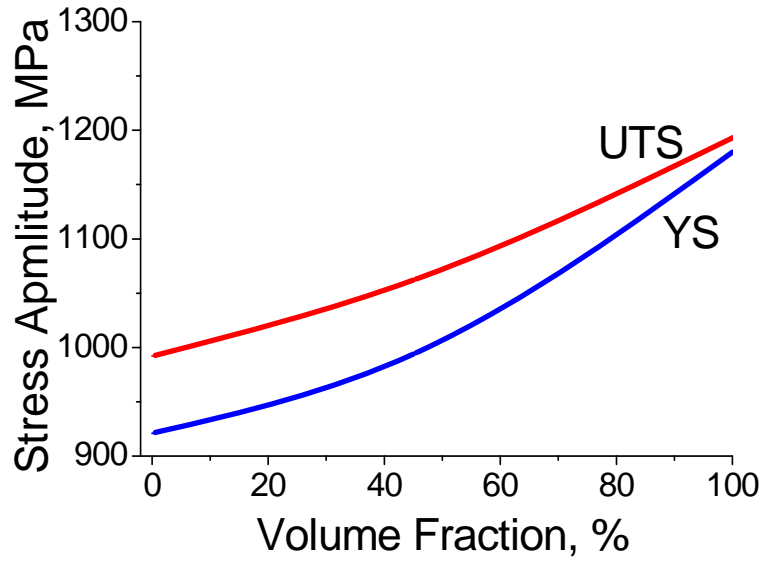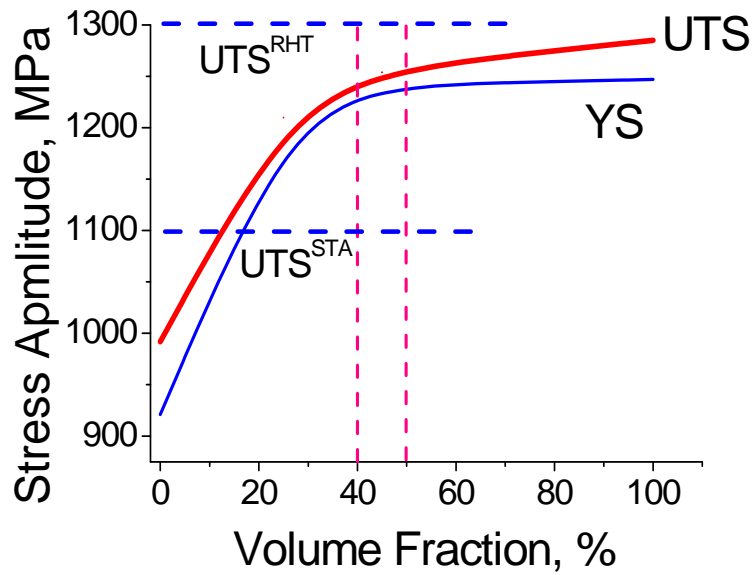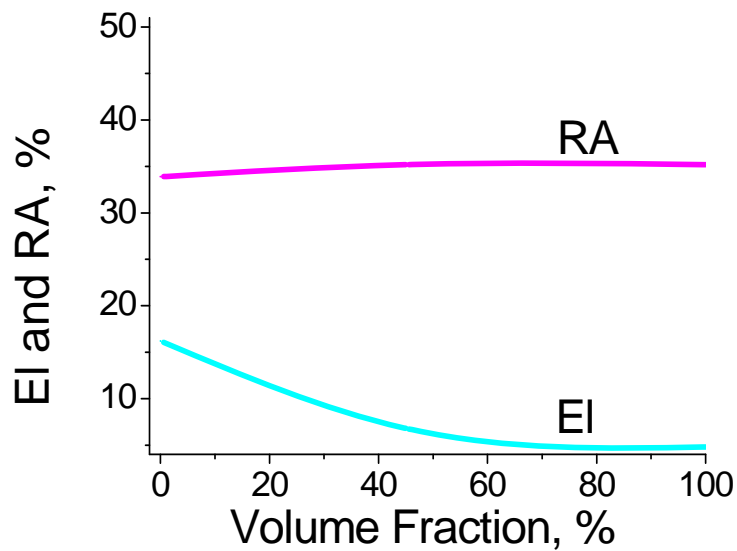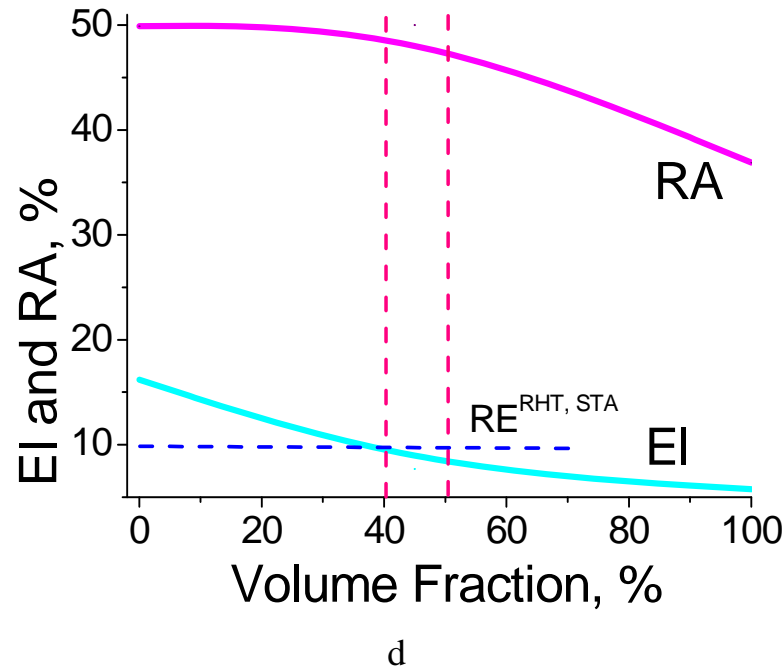
Fig. 23. Influence of transformed volume fraction of LRH-Treated material on Mechanical Properties of Ti-6-4 alloy. (a, c) – LRHT + WQ, (b, d) – LRHT + WQ + aging 550°C, 6h; (a, b) – Characteristics of Strength, (c, d) – Characteristics of Ductility.

Most important information about efficiency of LRHT for this alloy can be drawn from properties presentation of tensile data in the form given in Fig. 23, where strength and ductility properties are shown as functions of a volume fraction (VF) of heated above beta-transus material. So, for just LRH-treated and WQ condition (not aged) both strength characteristics monotonically increased with increase of VF (Fig. 23a), with decrease of relative elongation and relatively constant level of redaction in area (Fig. 23c). In case of strengthened by LRHT followed by aging condition fast growth of strength characteristics was observed in the range between 0 and approximately 40-50% of VF (Fig. 23b). On subsequent increase in VF rate of strength increase became much lower, whereas ductility decreases monotonically within a whole VF interval (Fig. 23d). Taking into account known for this alloy UTS levels for conventional (based on furnace heating) methods of STA-hardening, as well as for bulk RHT-hardening [13], and minimal permitted level of RE, it is possible to conclude following. Application of LRHT under the regimes ensuring formation of 40-50% in critical cross-section of beta-transformed material allows to obtain microstructural condition having strength at least by 25% higher than after conventional STA, that is balanced with approximately the same level of ductility. Despite the fact, that bulk RHT caused in a little bit higher UTS, proposed LRHT have important advantage because required essentially lower expenditures of energy, etc.

Fatigue testing data. Fatigue tests were done for Ti-6-4 alloy in reference condition having initial globular (annealed at temperature in α+β-field) microstructure and for LRH-Treated specimens. All results are presented in Fig. 24 and clearly represent advantages of LRH-Treated material over initial globular condition (fatigue limit is higher of about 70 MPa), which also was characterized by relatively high as for Ti-6-4 alloy fatigue limit. Taking into account obtained by us fatigue data for the same material [14] having similar bulk grain and very similar intragrain lamellar α+β microstructure (dashed line in Fig. 9) it is possible to conclude, that LRHT allows to reach the same high-cycle fatigue resistance like bulk RHT because of formation in surface layers microstructure of the same kind. This conclusion is rather rational and SEM study of fracture surfaces (Fig. 25) confirmed that fracturing cracks were formed on the surface of specimens. Difference between bulk and local (surface) RHT in this case consisted in lower low-cycle fatigue

resistance (at higher loaded stresses), when resistance against crack propagation is a main characteristic controlling the fracture. In other words, cracks propagate easily in gradiental microstructure contrary the same kind uniform one. At the same time presented in Fig. 24 dotted line represents lowest boundary of fatigue resistance for the same material having fine lamellar intragrain microstructure, but inside coarse (having average size more than 200 μm) grains. Field between this and dashed lines represents possible range of fatigue properties variation for Ti-6-4 with such a type of microstructure (beta-transformed fine-lamellar) depending on beta-grain size.

Summarizing all obtained results of mechanical properties testing for Ti-6-4 alloy with initial globular microstructure it is possible to underline, that LRHT allows seriously improve balance of tensile strength and ductility as well as fatigue resistance of studied material.
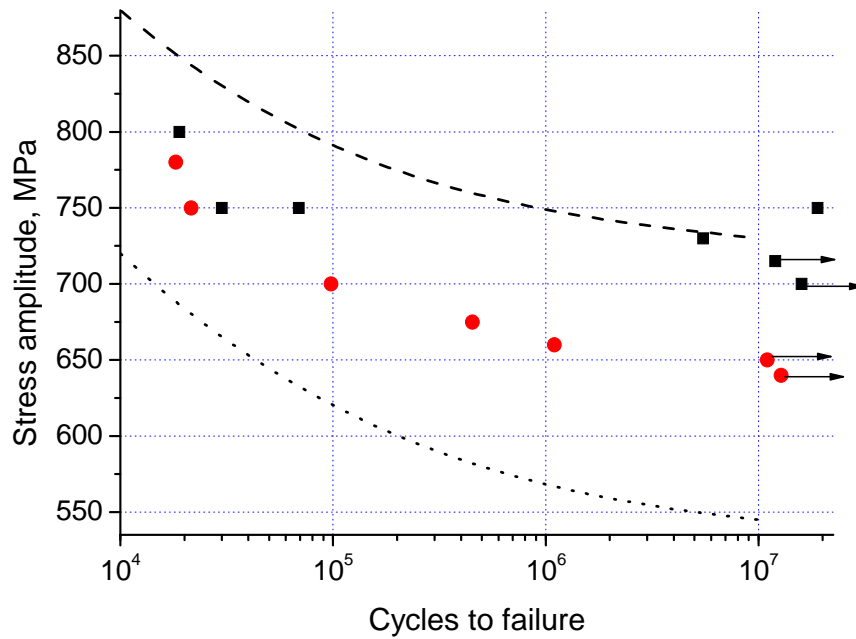
Fig. 24. S-N fatigue curves for Ti-64 with initial globular microstructure (round points) and after LRHT + aging (square points). Dashed line correspond Ti-64 alloy after bulk RHT and aging; dotted line – the same alloy after solid solutioning, quenching and aging, both results from [14].
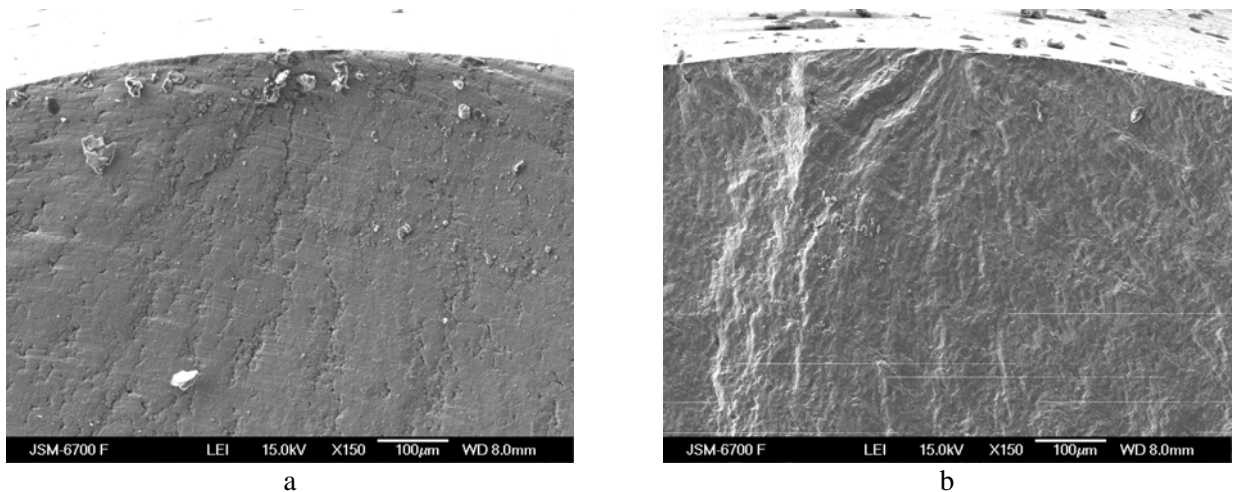
Fig. 25. Fracture surfaces of Ti-64 specimens fractured at 750 MPa in (a) initial globular condition and (b) after LRHT + aging. SEM.

4.2.2. Ti-6-4 alloy with initial lamellar microstructure.

Application of LRTH for improvement of initial lamellar microstructure, for instance – refinement of intragrain α+β lamellae, and, as a result possible improvement of some mechanical properties of α+β alloys looks like very attractive goal. That is why we annealed (in vacuum) some cylindrical specimens of Ti-64 at 1050°C during 1 h and formed coarse grained (with average grain size above 500 μm) lamellar microstructure (Fig. 26a). After LRHT under the regime 4 kW, 4 sec/WQ we don't observe any difference between core and surface layers in macrostructure and, what was more unexpectedly microstructure in all locations was also very similar to initial one (compare Figs.26b and c with 26a). At the same time X-ray diffraction analysis showed that whole specimens' volume was in martensitic α' – condition, i.e. undergoes sequences of α+β→β→α' transformations (Fig.27). From our point of view formation of such unusual martensitic microstructure is a result of uncompleted homogenization of high-temperature beta-phase on rapid heating when α'-crystals on quenching appeared repeating location of primary alpha-lathes.

a   b

c
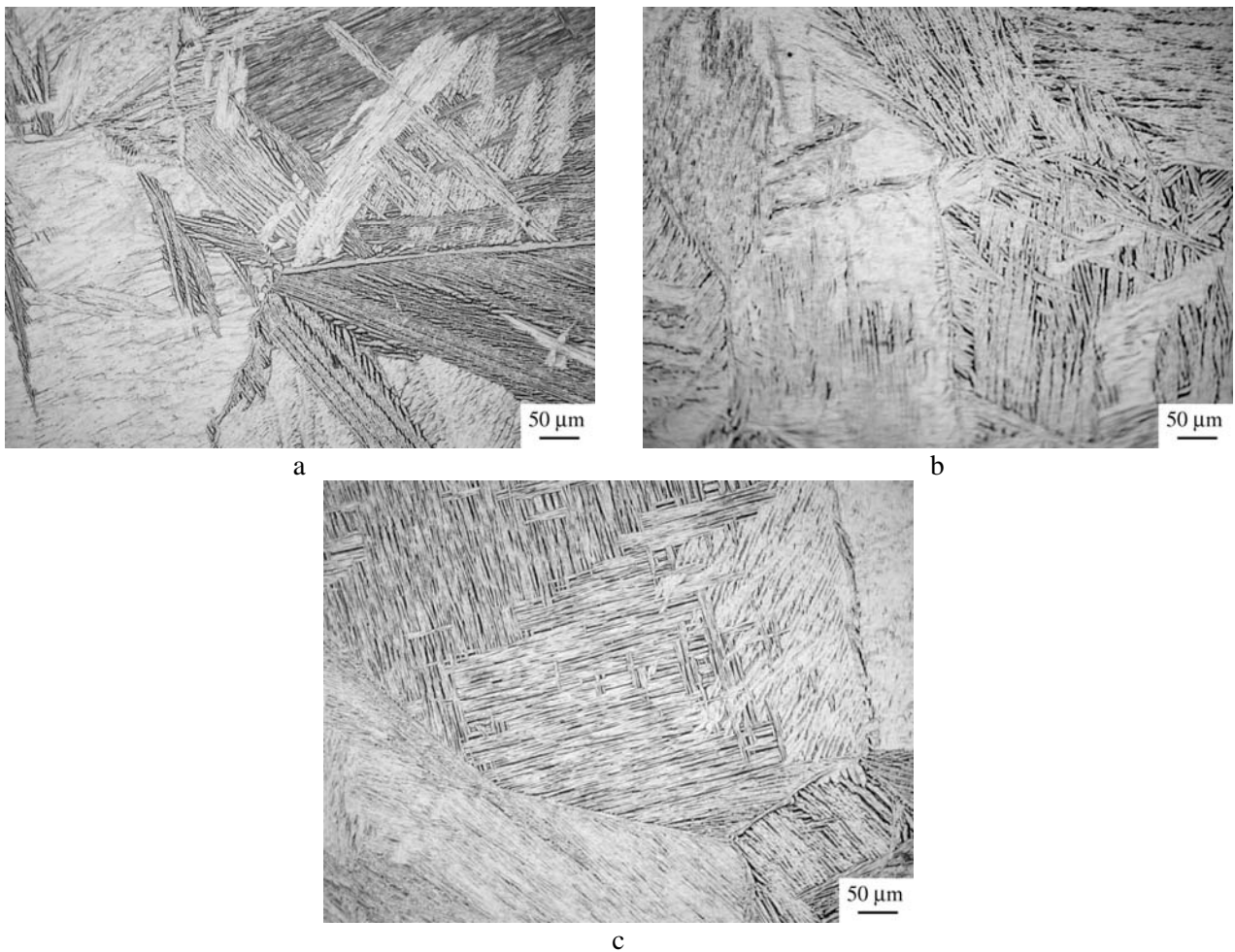
Fig.26. Microstructure of Ti-64 alloy with initial lamellar microstructure; (a) – initial annealed condition, (b, c) – after LRHT 4 kW, 4 sec/WQ; (b) – surface layer; (c) – core. LM, longitudinal section.

Increasing of treatment duration and, hence, duration of exposure at temperatures above T_{β}, obviously, caused in formation of more homogeneous high-temperature beta-phase since appeared on quenching martensite was relatively finer in all locations (Fig. 28a, b). But subsequent aging don't cause formation LM-visible finer α+β microstructure (Fig.28c).
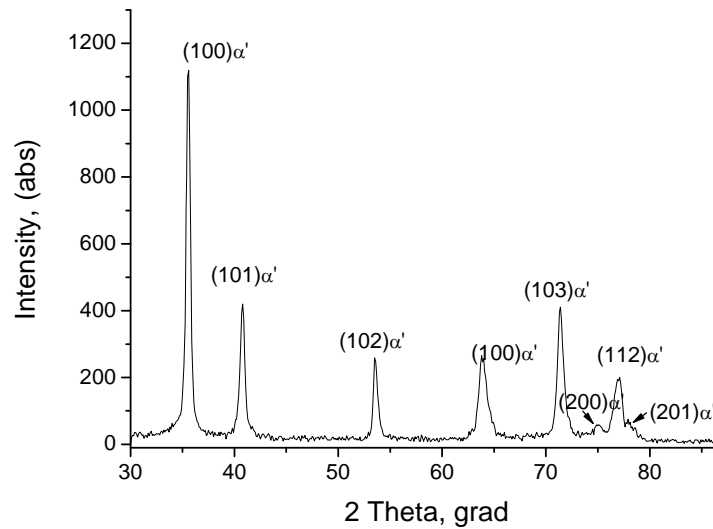
Fig. 27. Θ–2Θ X-ray diffraction pattern of Ti-64 alloy with initial lamellar microstructure after LRHT 4 kW, 4 sec/WQ.
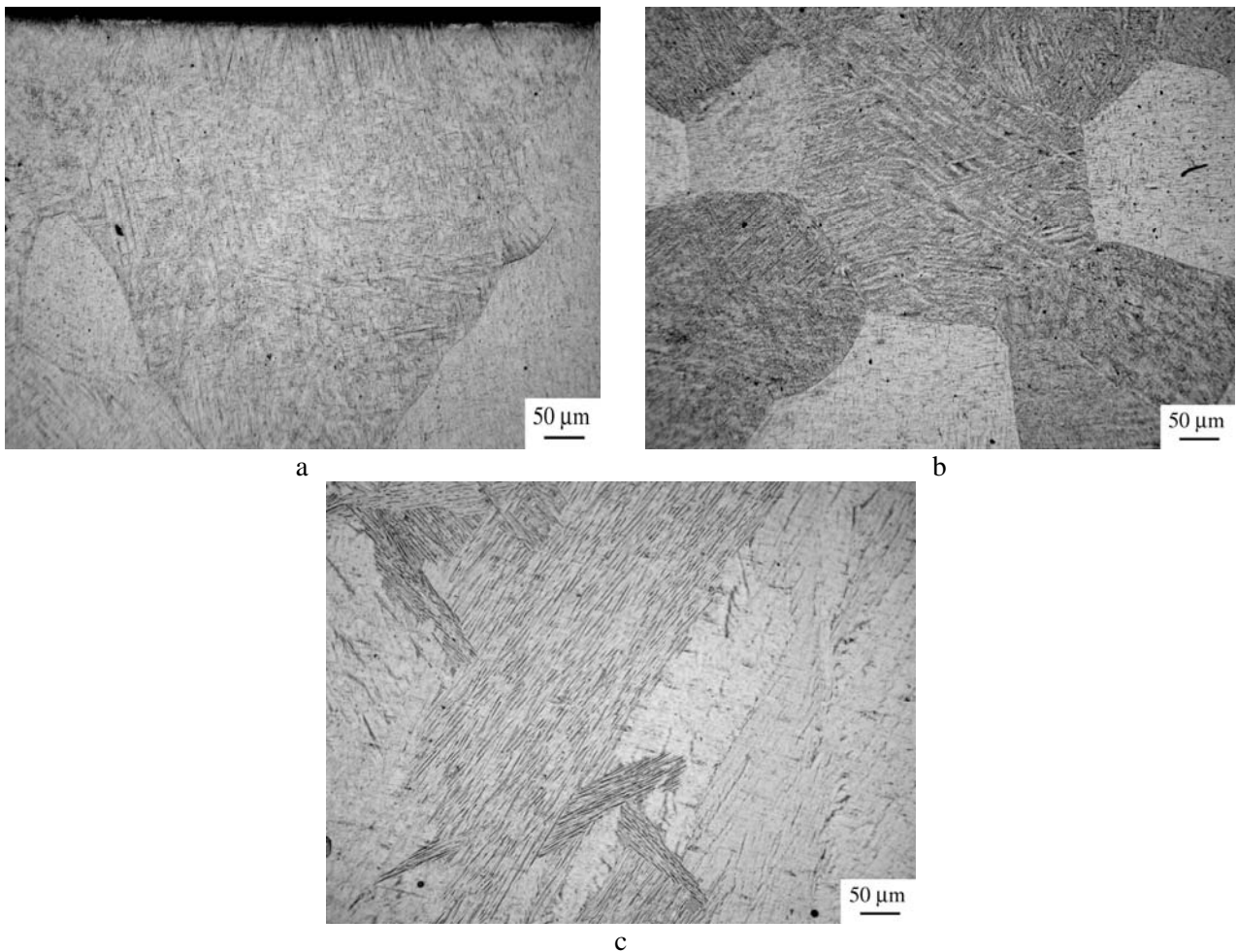
Fig. 28. Microstructure of Ti-64 alloy after LRHT 4 kW, 5 sec/WQ: (a, b) and after additional aging 550°C, 6h (c). (a, c) – surface layer; (b) – core. LM, longitudinal section.
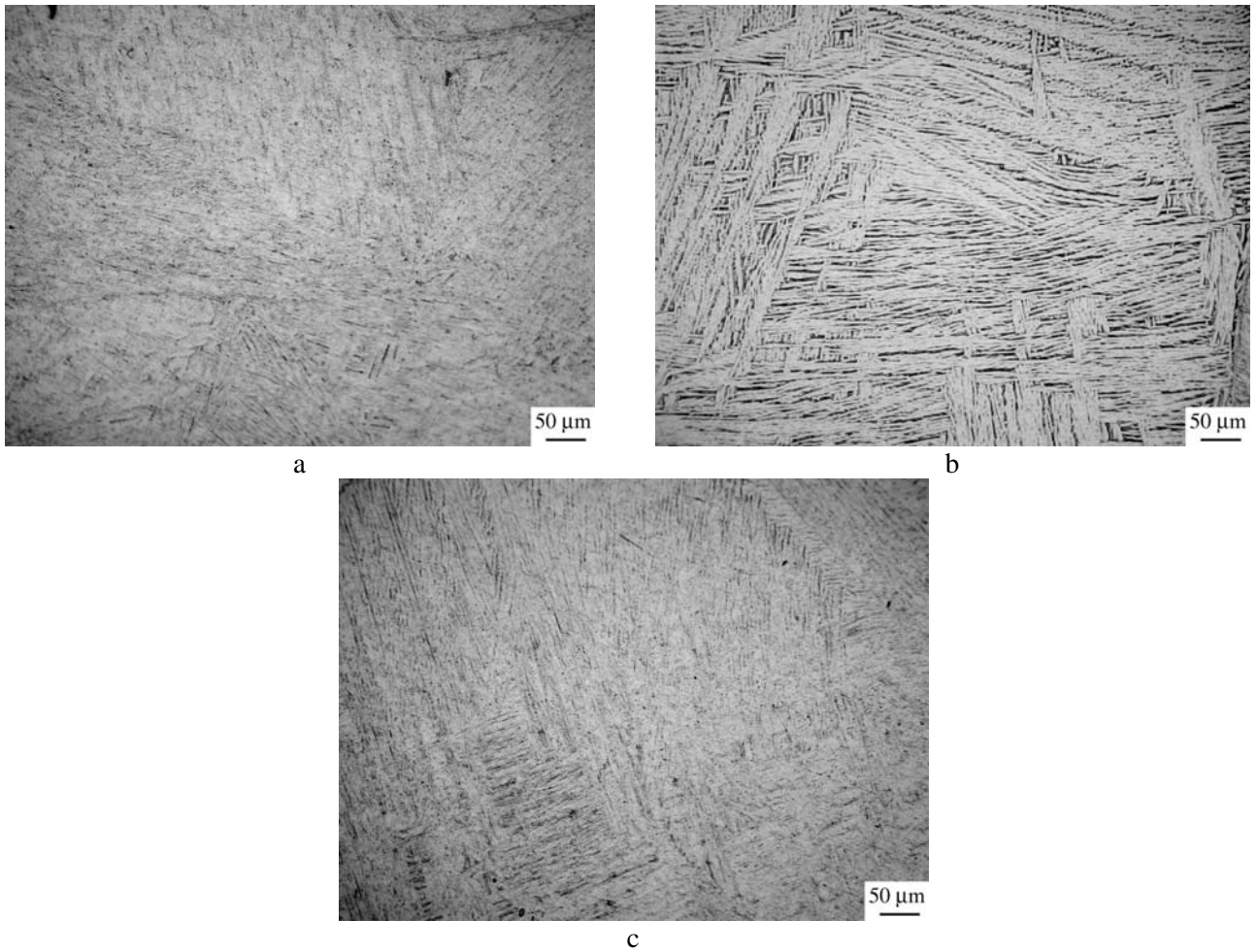
Fig. 29. Microstructure of Ti-64 alloy after double LRHT (4 kW, 5 sec/WQ): (a, b) and after additional aging 550°C, 6h (c). (a, c) – surface layer; (b) – core. LM, longitudinal section.

Double LRHT using regime 4 kW, 5 sec/WQ was performed to eliminate influence of strong inhomogeneity of high-temperature beta-phase on formed during its' decomposition α'- martensite. Obtained after such treatment and additional aging microstructures are shown in Fig. 29. Despite microstructures in Figs. 5 and 6 in all locations look very similar, tensile tests of two types of aged specimens (after single and double LRHT) showed, that exactly double LRHT allows to obtain better balance of tensile strength and ductility as compared with initial lamellar as well as single-LRH-Treated material (Table 3).

Table 3

Mechanical Properties of Ti-64 (initial lamellar condition) after different treatments

##	Condition	Volume fraction heated above T_β, %*	Tensile properties			
			YS, MPa	UTS, MPa	El, %	RA, %
1	Initial, annealed 1050°C, 1h/FC	0	867	933	9.05	25.8
2	+ LRHT: 4kWt, 5 sec/WQ: +550°C, 6h	100	1190	1205	5.82	28.6
3	+ LRHT: 4 kW, 5 sec/WQ(x2) +550°C, 6h	100	1182	1199	8,17	32,3

* Gage Ø 4 mm was taken into consideration.

4.2.3 LRHT of titanium beta alloy (TIMETAL-LCB).

Investigations of phase and microstructural transformations in beta-titanium alloys during LRHT were done using TIMETAL-LCB as an object of study. First of all we evaluated temperature distribution through specimen employing earlier proposed experimental/calculation method. Obtained results are presented in Fig. 11c. Comparing with earlier obtained for Ti-6-4 and the same applied power data it is possible to mention, that in the present case similar treatments caused in a little lower temperatures in all locations, as compared to case of CP-Ti and Ti-6-4 (compare Figs. 11c with 11a and 11b).

Taking into account peculiarities of titanium beta alloys [15, 16] TIMETAL-LCB was solid-solutioned (900°C, 30'), water quenched to obtain completely metastable beta-condition (Fig.30a), than cold drawn with total plastic deformation 90% (Fig. 30b). This heavy deformed condition was used as initial for subsequent LRHT application aimed to obtain recrystallized fine beta-grain microstructure in surface layers like in whole material after application of bulk RHT [15, 16]. Degree of recrystallization and depth of its penetration were varied using different duration of treatment.

a	b
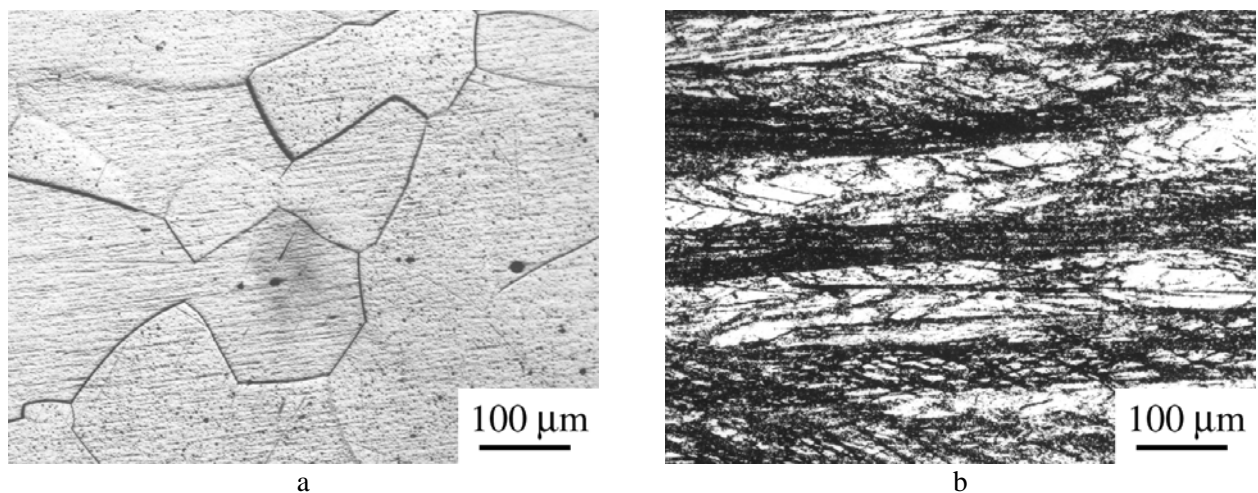
Fig. 30. Microstructure of TIMETAL-LCB after: (a) – solid solutioning at 900°C during 30' and water quenching, and (b) – subsequent 90% cold deformation. LM.

Surface layer   Centre (Core)

a	b
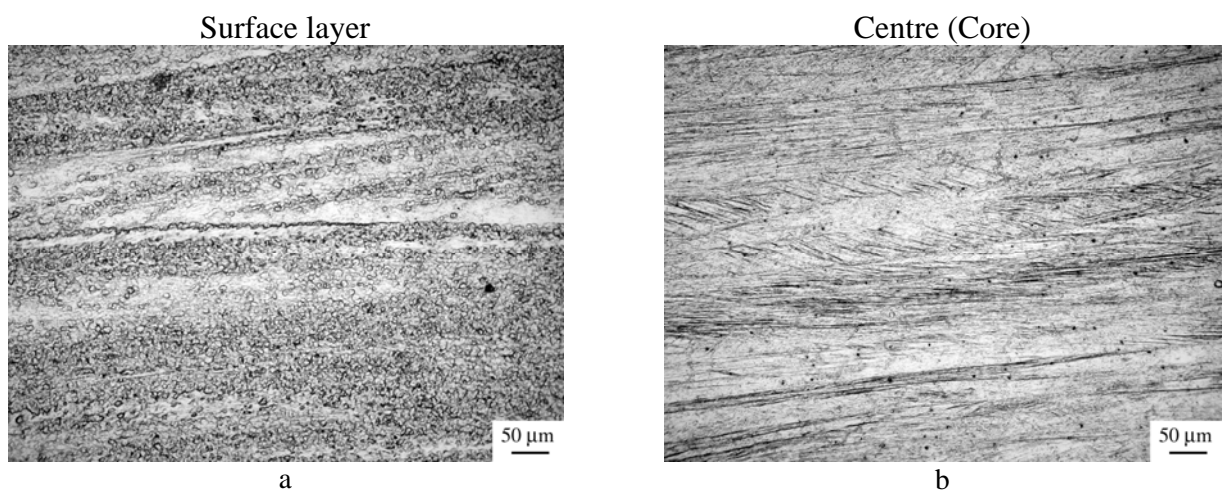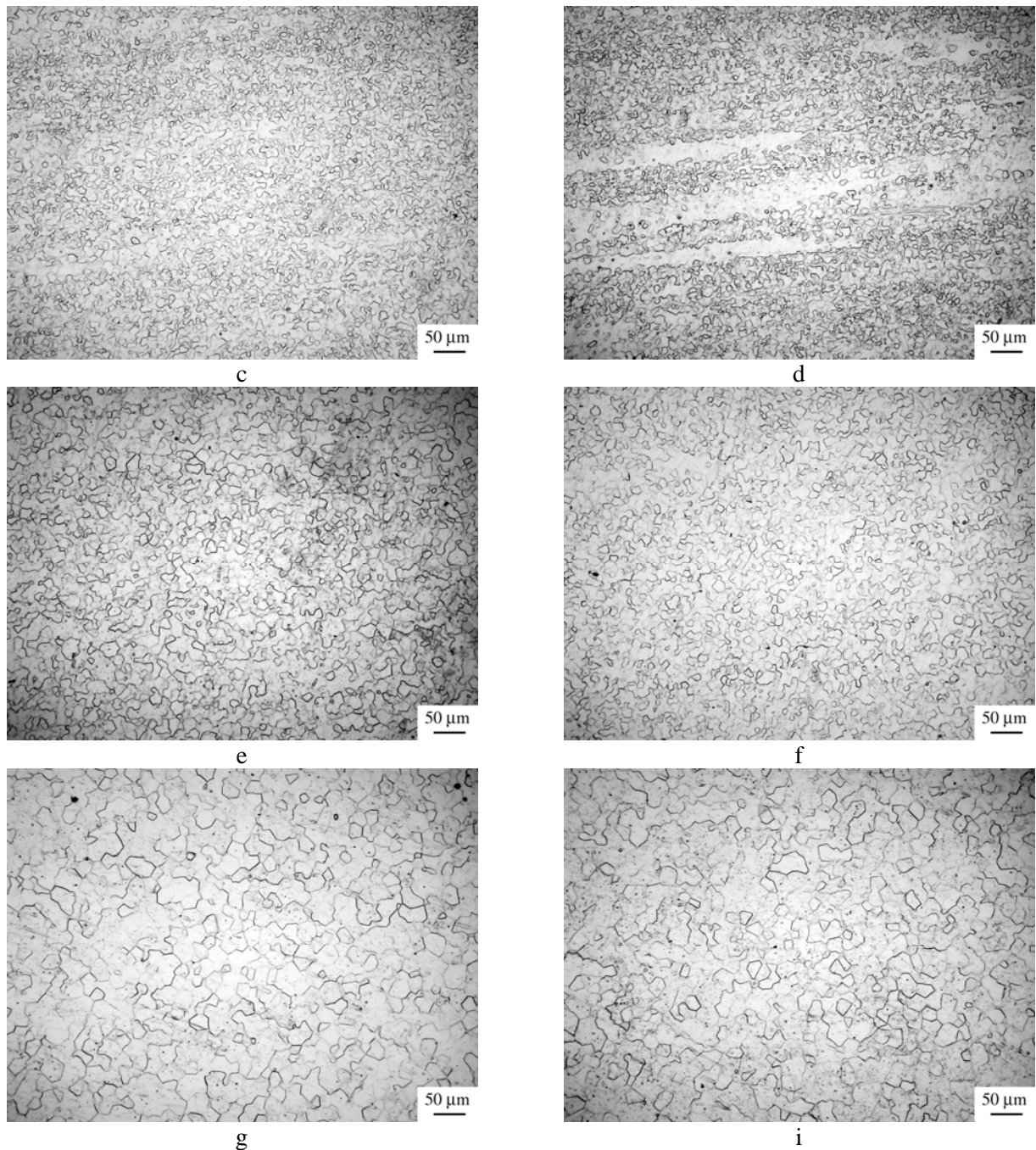
Fig. 31. Microstructure of TIMETAL-LCB after LRHT 4 kWt during: (a, b) – 2.5 s, (c, d) – 2.7 s, (e, f) – 3.0 s, (g, i) – 3.3 s. (a, c, e, g) – Surface layer, (b, d, f, i) – Centre (Core). LM.

Typical examples of obtained microstructures are shown in Fig. 31 and clearly represent microstructure evolution in two locations (surface and core) versus duration of LRHT. According temperature curves from Fig. 30 first sings of recrystallization became visible in the surface layer after reaching 820°C, that is very close to earlier obtained for the same alloys and conditions of bulk RHT [15]. Increase of LRHT duration from 2.5 s to 2.7 s caused in finishing of recrystallization in surface layer and more than 50% development of recrystallization in core due to relevant increase of temperature (Fig. 31c and d, and see corresponding curve in Fig. 11c). Recrystallization in all locations was completed after 3.0 sec LRHT (Fig. 31e, f) and further increase of treatment duration caused in coarsening of beta-grain microstructure (Fig. 31g and i), but some difference in grain size between surface layer and core remains for all durations of LRHT. So, application of LRHT allows to obtain in deformed titanium beta-alloys recrystallized conditions with fine beta-grain microstructure, that also has some variation in grain size.

Mechanical (tensile) properties were measured for some microstructural conditions (Table

4). Fig. 32 represents comparison of Strain-Stress curves for completely recrystallized and finally aged specimens.
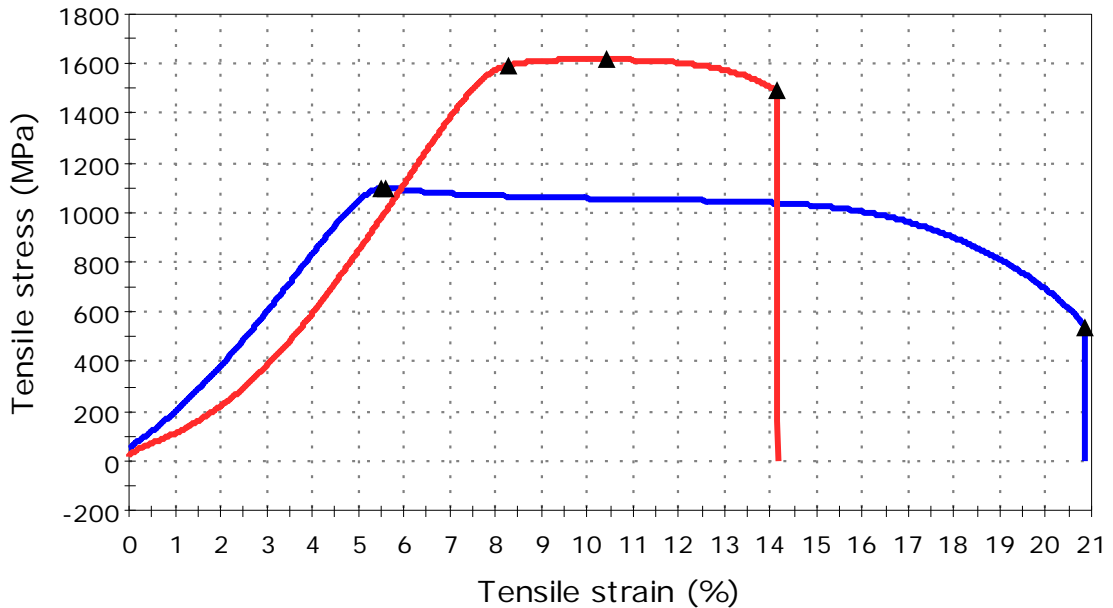
Fig. 32. Technical Stress-Strain curves for TIMETAL-LCB in recrystallized with LRHT (4 kWt, 3 s; blue curve) and recrystallized + aged 520°C, 8 h (red curve) conditions.

Table 4
Tensile properties of TIMETAL-LCB in different conditions

##	Condition	YS, MPa	UTS, MPa	Elongation, %	RA, %
1	90% Cold Deformation	1377	1465	11,56	63,82
2	+ LRHT 4kWt, 3 s	1095	1097	17,57	73,46
3	+ LRHT 4kWt, 3 s +520°C, 8h	1615	1650	5,57	17,56
4	*RHT+520°C, 8h [15]*	*1600*	*1640*	*9,4*	*36,5*
5	+ LRHT 4kWt, 2.5 s +538°C, 8h	1569	1587	6.57	24.47
6	+ LRHT 4kWt, 2.7 s +538°C, 8h	1481	1512	7.03	27.48
7	+ LRHT 4kWt, 3 s +538°C, 8h	1445	1502	7.91	29.59
8	+ LRHT 4kWt, 3,3 s +538°C, 8h	1441	1501	6.15	24.48
9	*RHT+538°C, 8h [15]*	1480	1510	10.5	43.0

As can be seen from presented tensile data even heavily cold drawn TIMETAL-LCB has a good combination of tensile strength and ductility (#1 in Table 4). After LRHT material became much softer (#2 in Table 4, and blue curve in Fig. 32), while after final annealing (##3, 5 – 8 in Table 4 and red curve in Fig. 32) this alloy is characterized by very high strength and reduced a little ductility. Comparing these results (#3 and 6) with earlier obtained (#4 and 9) for the same alloy employing bulk RHT data [15] it is possible to conclude, that after LRHT received level of strength characteristics is a little higher, but characteristics of ductility are noticeably lower. Such a situation may be, in first approximation, explained by some difference in microstructure, namely – in case of LRHT application gradual (through specimen diameter) microstructure was formed; subsequent aging probably increases such a difference. Special attention should be paid to the conditions having not recrystallized core (##5 and 6) because in this case the deformed β-phase, that has a lot of residual deformation defects, was aged, and resulting level of strength is visibly

higher. Nevertheless, obtained after LRHT and aging result looks rather good and during the next quarter we will try to find more optimal regimes of this treatment as well as final aging to obtain better balance of properties.

4.3. LRHT of turbine engine compressor blades.

According to the project working plan research activities aimed on selection of optimal regimes of titanium blades made of VT8 alloy (having actual composition Ti- 6.7(wt.%)Al - 2.9Mo) LRH-Treatment were performed. First of all, for developed inductor (see Fig. 6,) dependence between heating regimes and temperatures distribution obtained was studied. Variable parameters of LRHT were duration of treatment and method of cooling after heating finishing – water quenching (WQ) of air cooling (AC). Typical examples of LRH-Treated blades general view presented in Fig. 33, and results of temperature distribution during LRHT measured with pyrometer are shown in Fig. 34. It is necessary to underline, that due to very small diameter of spot measured by pyrometer every temperature map in Fig. 34 is a result of at least 15 experiments on blade heating under the same regimes. Since thickness of blades in heated zone varied around 2 mm (the depth of generated heat at 400 kHz induction heating layer was earlier estimated as 1.2 mm) and heating was performed from both sides, it was concluded that temperature inside the heated body was uniform and equal to measured on the surface values. Taking into account these data treated via different regimes blades were cut into several specimens for X-ray diffraction analysis to check phase composition and LM examination of microstructure in two perpendicular directions as shown by arrows in Fig. 34b.

a   b
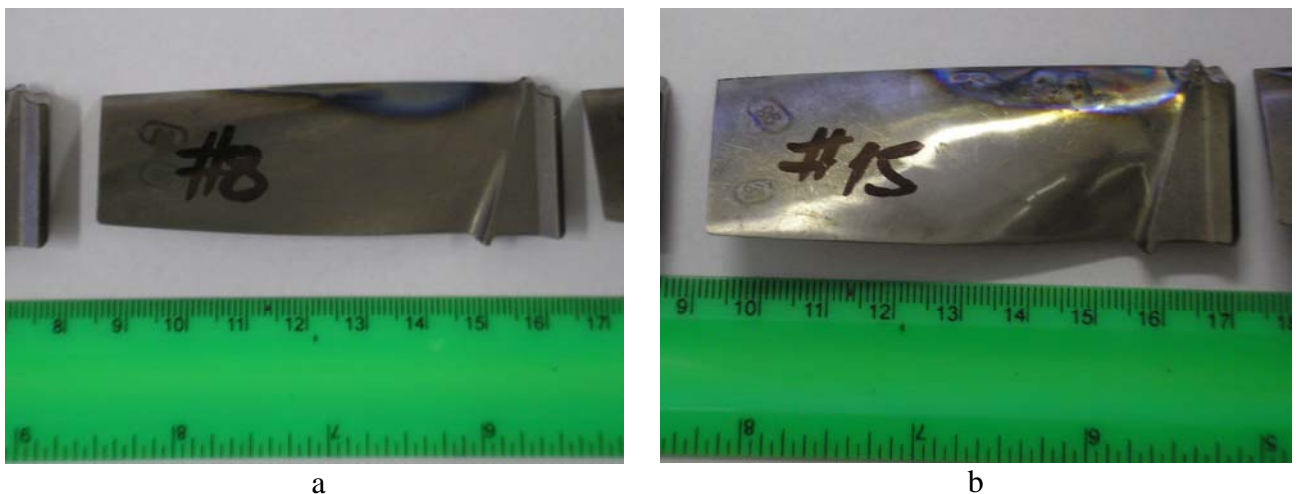
Fig. 33. Typical examples of LRH-Treated blades. LRHT regimes: (a) – 5 kWt, 2.5 sec/WQ; (b) – 5 kWt, 3.0 sec/AC.

a

b
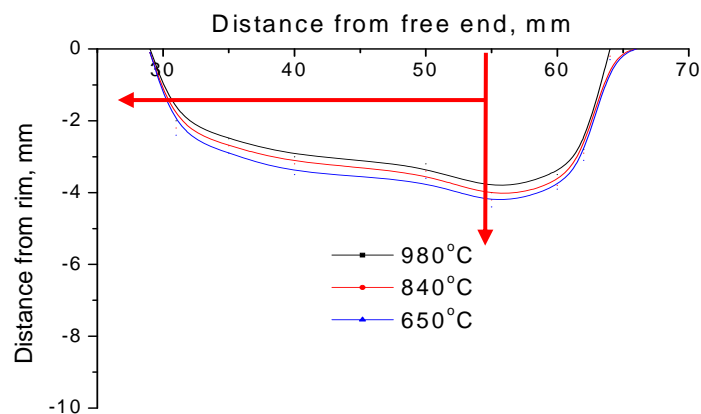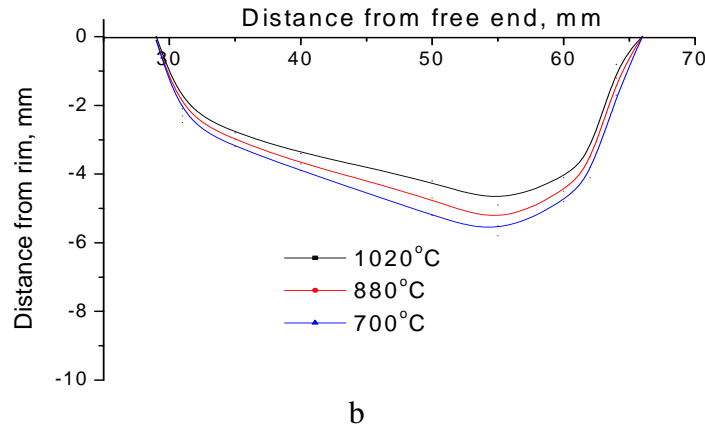
Fig. 34. Typical temperature distribution in LRH-Treated zone of blades. LRHT regimes: (a) – 5 kWt, 2.5 sec; (b) – 5 kWt, 3.0 sec. Arrows on Fig.33a correspond to directions in which blade was cut for phase composition and microstructure characterization.

Main method employed for blades' testing of blades in both initial (as received from manufacturer), and after LRHT conditions was method of fatigue tests with cycling banding on resonance frequency, as more corresponding to real working conditions of blades' operation. Principal scheme of testing is shown in Fig. 35. Electrodynamic vibrating unit UVE-5/3000 [2] was employed for testing. Vibration form the generator (1) was transmitted through the table and special holders to the blade (3) initiating in it transverse banding waggling under symmetric cycle. An amplitude of wagging of blade free end was measured during tests, and strain sensor was glued to the gage section of blade for estimation of relationship between amplitudes of free end oscillation and applied stresses. First of them was measured using light microscope MBS-2 with ocular micrometric scale; number of cycles and frequency of waggling was controlled with electronic frequency counter ChZ-34 [17]. The value of main reduced error of measurements was not more than ± 1%. Decrease of resonance frequency of tested blade more than by 1% was taken as a criterion of its failure. This situation corresponded to formation of surface macrocrack having depth of about 0.5 mm.
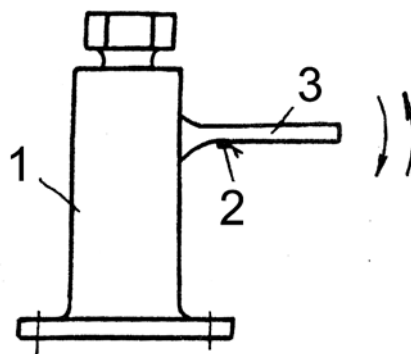
Fig. 35. Scheme of blades testing: 1 – electrodynamic vibrating unit, 2 – strain sensor, 3 – tested blade.

During fatigue tests unexpectedly, we found, that the main location where fatigue cracks were initiated was blades' convex face (Fig. 36a), while in monograph [18] authors established, that at least 50% of fracture in similar type blades and the under the same testing conditions should initiated on leading edge. In our case such situation was occur in one blade only (Fig.36b).
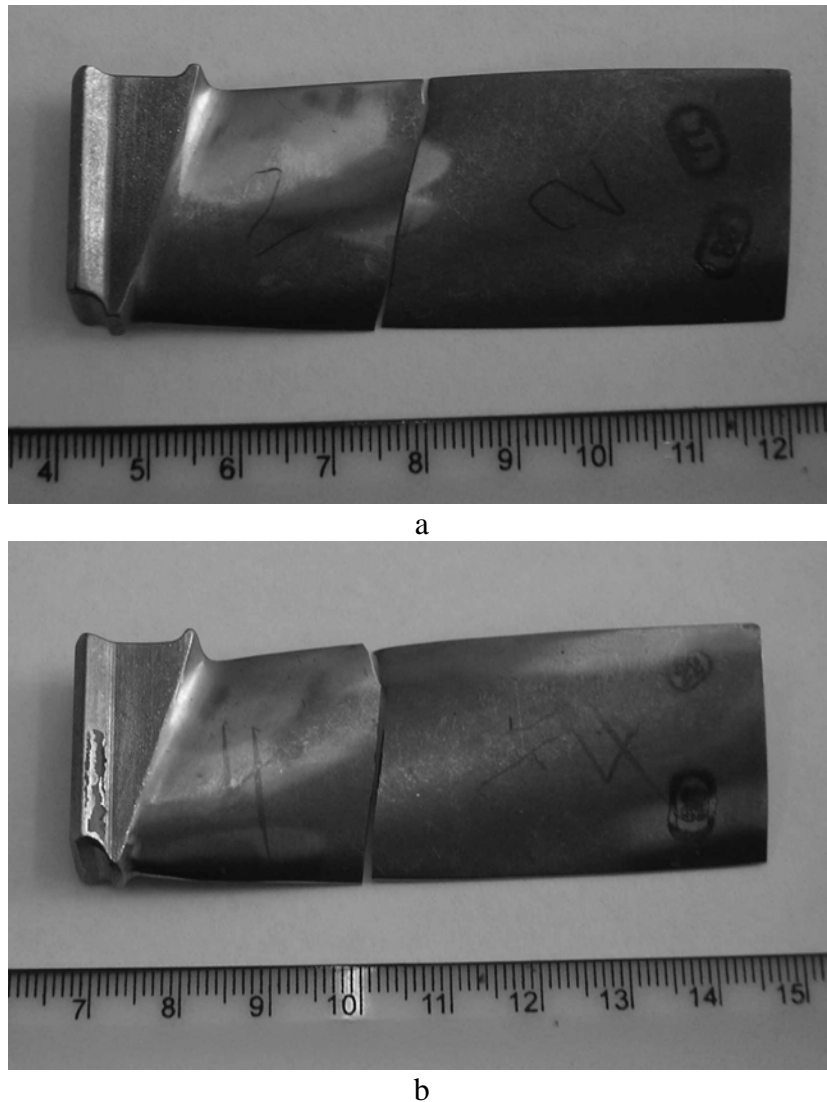
Fig. 36. Typical examples of blades in the initial as-received condition after fatigue testing. (a) – fracture from blades' convex face, (b) –fracture from leading edge.

SEM study of fractured blades showed, that in both cases fatigue cracks were nucleated below the blades' surfaces (Fig. 37a, c), and then propagated very quickly through a whole blade cross section (Fig. 37b, d). Reason of such an effect is applied by producer for blades strengthening technology of shot peening employed as one of finishing stages [19]. From one hand, this fact explains relatively high level of fatigue strength, but from another, means, that any subsequent heat treatment (LRHT including) should cause in removal of this residual stresses. So, having as a goal improvement of fatigue properties with LRHT, we have to form in blades such structural condition in which increase in fatigue resistance could be visibly higher comparing with its reduction related to elimination of shot peening effects. This purpose required to apply LRHT to both critical locations of blades – to leading edge, as well as to convex face. As for the last case, it was suggested, that LRHT employment required designing and preparation of a new special kind inductor (see Fig. 6b).

Another conclusion made on the base of above result consists in following. It is known, that formation of even small defects (scratches, nicks and other types of shallow stress concentrators) during engines exploitation is a serious problem reducing fatigue life of blades [20, 21]. At the same time in several works [7, 8] it was shown, that fine-grained β-transformed microstructure in titanium two-phase α+β alloys should have superiority over some others microstructural conditions (including globular one – Fig. 38) in fatigue life because of better resistance against crack nucleation and propagation. That is why we proposed to perform comparative testing of blades with surface stress concentrators cut on the leading edge of blades in two principal conditions: i)

reference, i.e. initial having globular microstructure, and ii) after LRHT and standard for this alloy aging forming fine-grained β-transformed microstructure.
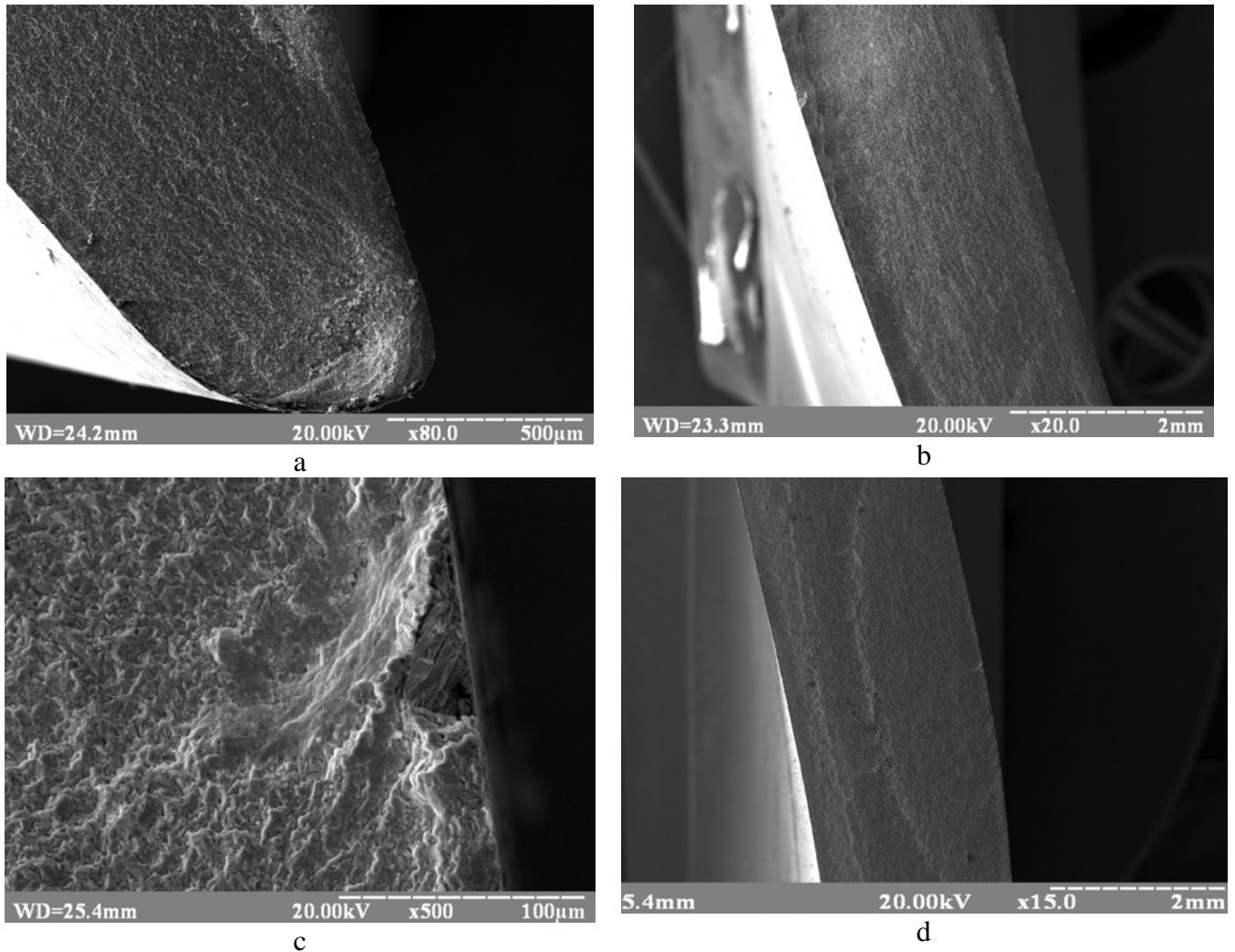
Fig. 37. Fracture surfaces of blades after fatigue testing. Fracture initiated from: (a, b) – leading edge; (c, d) – blades' convex face. SEM.
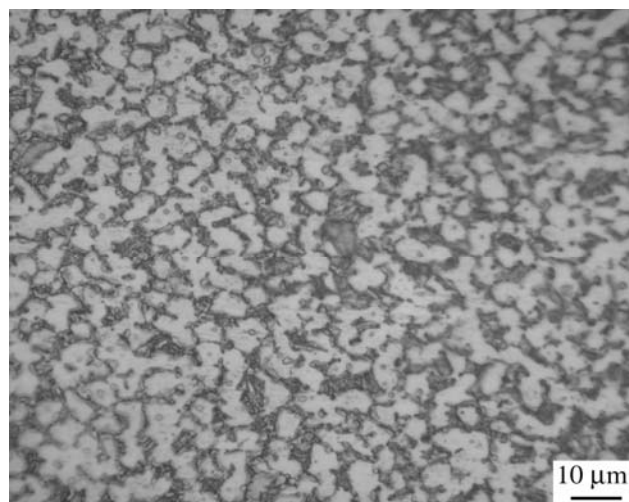
Fig. 38. Microstructure of blades in the initial condition. LM.

General view of blade cross-section after LRHT of leading edge is presented in Fig.39. It is

clear seen four different zones: (A) – not affected by LRHT having initial microstructure (Fig. 40), (B) – slightly affected by LRHT with a little reduced size of primary α-phase and increased amount of β-matrix between them (Fig. 40a), (C) – transition zone continuation where initial globular microstructure gradually transforms into (D) – completely β -transformed zone (Fig. 40b). It is necessary to underline, that in LRH-Treated zone average grain size doesn't exceed 50÷80 μm (Fig. 40b and c). Intragrain microstructure is so dispersed, that even after standard aging α+β-microstructure cannot be resolved with LM (Fig. 40c, - see analogous data in Figs. 18 and 19 for Ti-6-4 alloy).
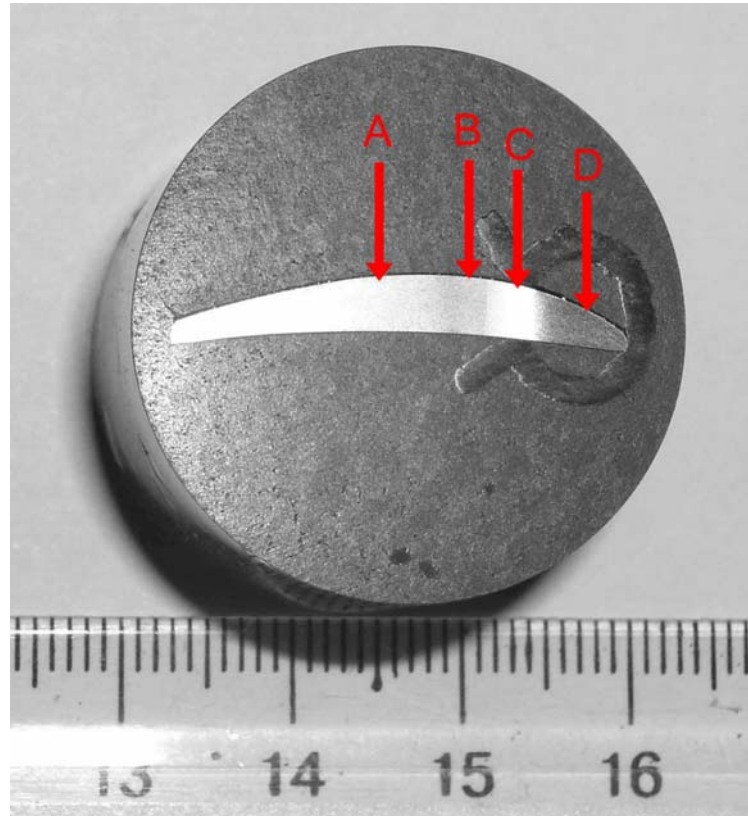
Fig. 39. Macrostructure of blade cross-section after LRHT: 5 kWt, 3 sec.
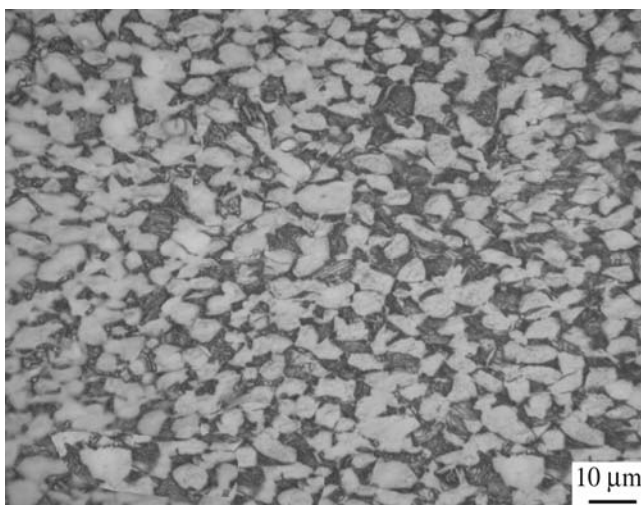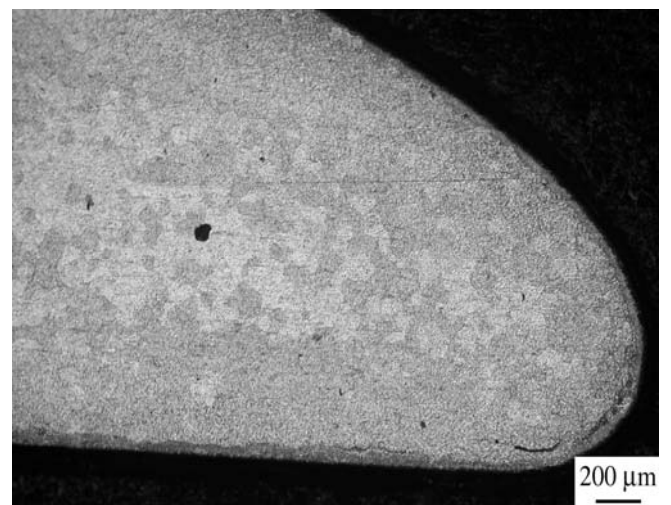
a   b
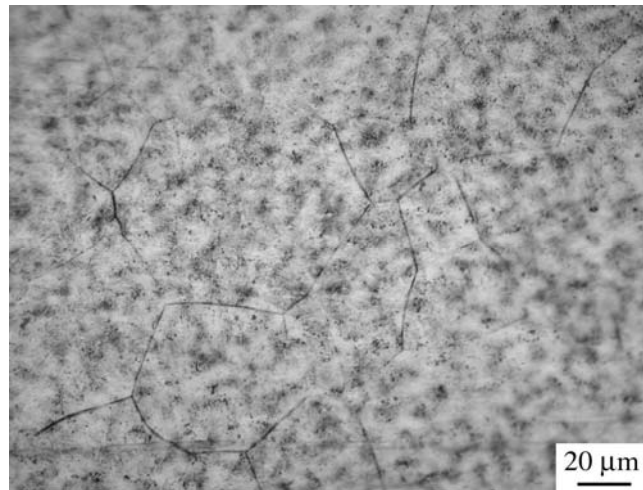
c

Fig. 40. Typical microstructure of blades after LRHT 5 kWt during: (a) – 2.5 sec, (b, c) – 3 sec + aging 550°C, 10 h. LM.

Fatigue tests of blades in LRH-Treated (both sides – leading edge and convex face, followed by final aging 550°C, 6h) conditions were performed. General view of typical examples of this type blade is shown in Fig. 41a, while after LRH-Treatment of leading edge is presented on Fig. 41b. Obtained fatigue data for both conditions (initial and after double LRHT) are shown in Fig.42. Fatigue stress limit of the first condition was estimated as of about 540 MPa; for the second one – 630 MPa. It is important to underline, that most pronounced advantage of LRHT condition (of about 100 MPa in fatigue limit) was observed for exactly high-cycle loading, whereas difference in low-cycle fatigue was essentially lower. The reason of this is presence of residual stresses in blades introduced by special surface vibro-acoustic treatment (of shot peening type) [19]. So, application of LRHT, from one hand – forming small-grained beta-transformed microstructure, from another hand – caused in reduction of these residual stresses. These two affects putted together and result of their superposition led to shown in Fig.42 improvement of fatigue properties, where higher effect for high-cycle loading is very similar to one earlier observed for round specimens of Ti-6-4 alloy.
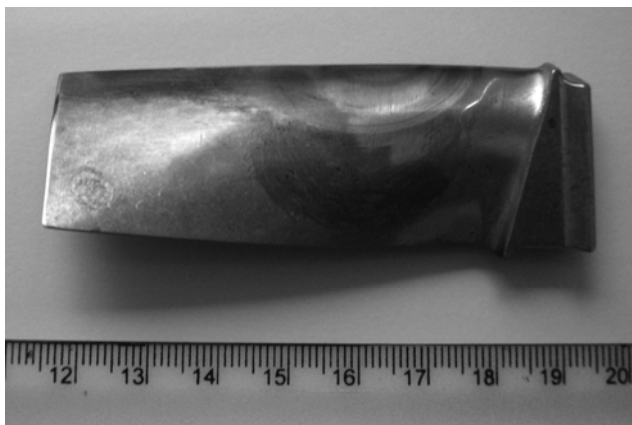
Fig. 41. Compressor blades after (a) double-LRHT and (b) LRHT of leading edge and final aging 550°C, 6h.

Also more detailed TEM study of fine microstructure of blade material after LRHT was performed. Typical results are shown in Fig.43. It is interesting to note, that air cooling after LRHT caused in formation a little finer martensite, as compared with water quenching (compare Fig. 43b and 43c). This is result of martensitic transformation realization under conditions of partial diffusional redistribution of alloying elements [22].
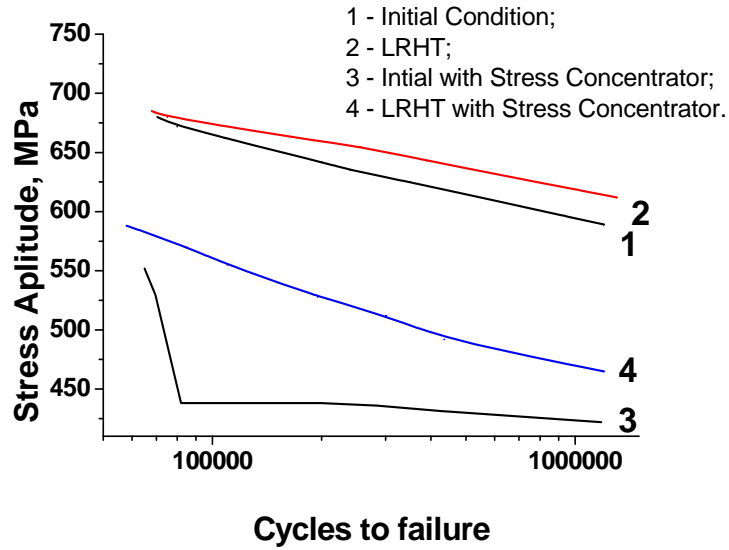
Fig. 42. S – N curves of VT8 compressor blades in different conditions (shown in Figure).

At the same time in the transition zone (where peak heating temperature was lower than T_β) bi-modal microstructure (with inclusions of residual α-particles) was observed (Fig. 43c), what also is very similar to results obtained for round specimens of Ti-6-4 alloy (see Chapter 4.2.1).
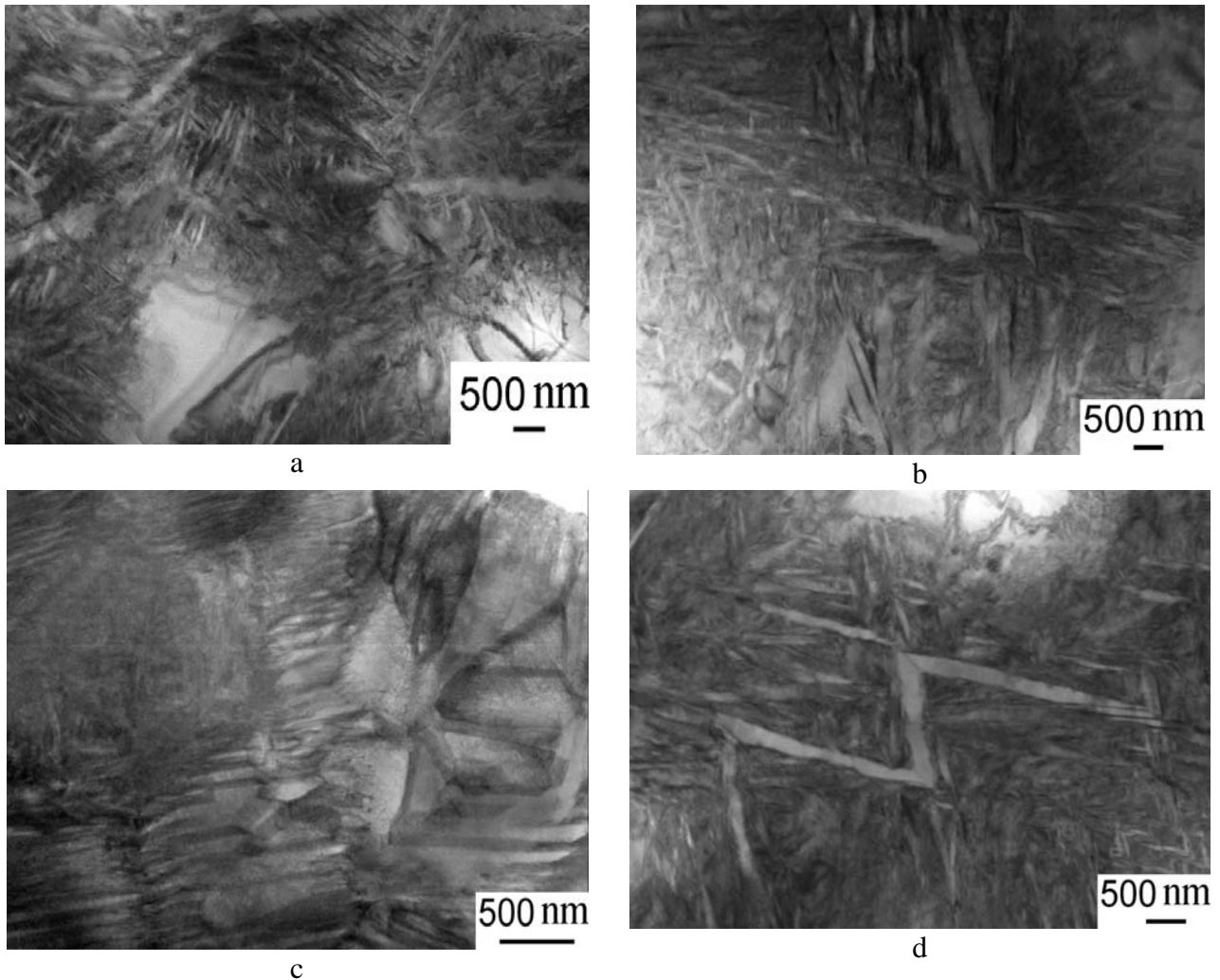
Fig. 43. Microstructure of compressor blades after LRHT and (a, b) – air cooling, (c, d) – water quenching. After cooling final aging 550°C, 6h was applied. TEM.

For investigation of stress concentration influence on fatigue performance of compressor blades concentrators with following parameters were cut: depth **h**=0.6 mm, radius **r**=0.2 mm (according approach developed in [18], as more adequate to real situation appeared on engine service). Three batches of cut blades were prepared: i) in the initial condition (Fig. 44a), ii) after LRHT followed by air cooling (AC, Fig. 44b) and iii) after LRHT followed by water quenching (WQ, Fig. 44c, d; for conditions ii) and iii) final stage of applied treatment was aging 550°C, 6h). As a result of fatigue testing it was found, that for two first conditions cracks were always initiated from stress concentrator (Figs. 44a and b), while for condition obtained with LRHT/WQ in the part of blades fracturing cracks appeared not in stress concentrator locations (Fig. 44c).

a   b

c   d
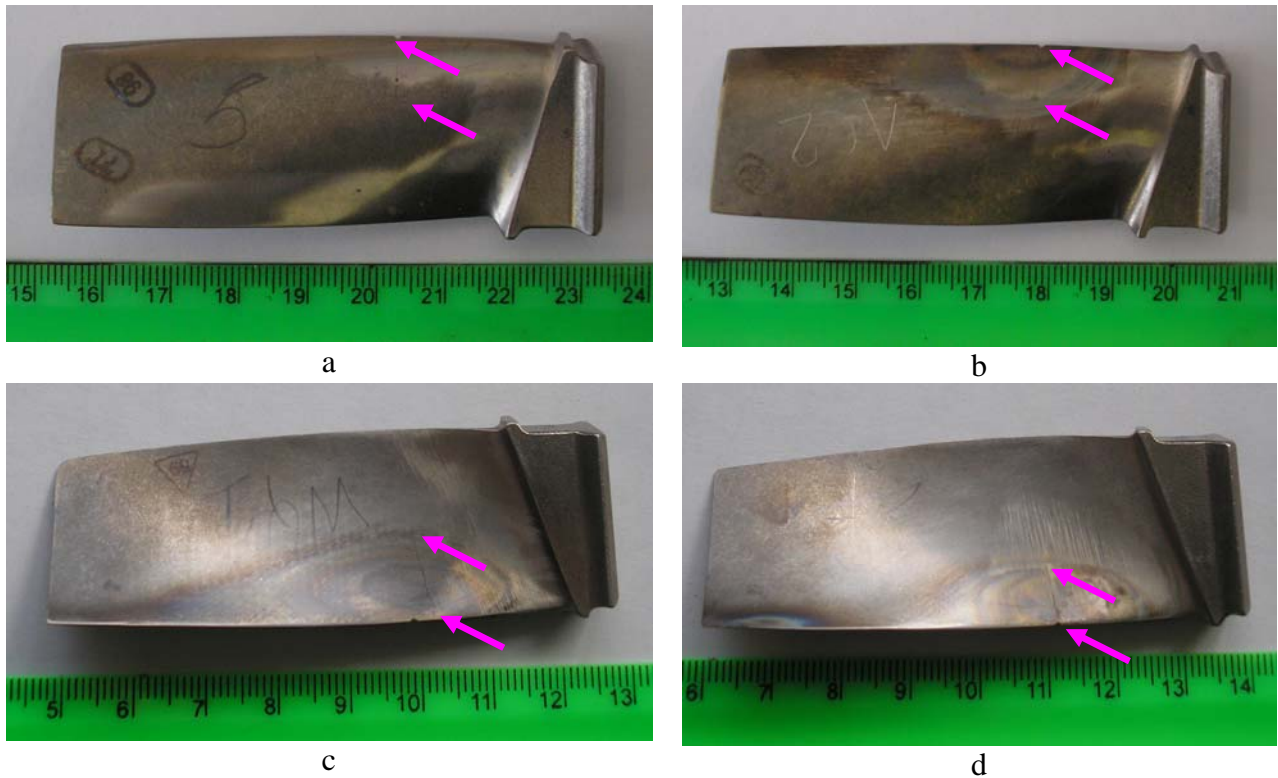
Fig. 44. General view of compressor blades with cut stress concentrators; (a) – initial condition, (b) – LRHT/AC + aging, (c, d) – LRHT/WQ + aging, (c) – fracturing crack appeared outside stress concentrator, (d) - fracturing crack appeared from stress concentrator. Arrows indicates location of fracturing cracks.

Results of these fatigue tests are also presented in Fig. 42. First of all necessary to note, that in both cases for notched and un-notched blades LRHT caused in improvement of fatigue behavior as compared with blades in initial condition. For blades without stress concentrator increase in fatigue resistance for LRHT blades was higher for high-cycle fatigue, whereas at low-cycle loading there was no serious difference observed. This fact is not usual for comparison of equiaxed and β-transformed conditions and may be explained by presence of residual compressing stresses introduced into initial blades with applied by producer ultrasonic-vibration surface treatment [19]. Application of LRHT removes this positive influence owing to phase α+β→β transformation, but at the same time it changes type of microstructure improving mechanical properties. So, final level of fatigue properties after RHT represents some superposition of these two effects and explains relatively small increase in highcycle fatigue strength (compare curves 2 and 1). Cutting of stress concentrator led to situation, when fracturing blade crack appeared in zone located below compressed by residual stresses layer, and in this case introduced by LRHT effect is much higher (compare curves 4 and 3).

Fracture surfaces of cut blades after fatigue testing are shown in Fig. 45. First of all it is necessary to note, that in all cases when fracture was initiated from stress concentrator (Figs. 45a-c)
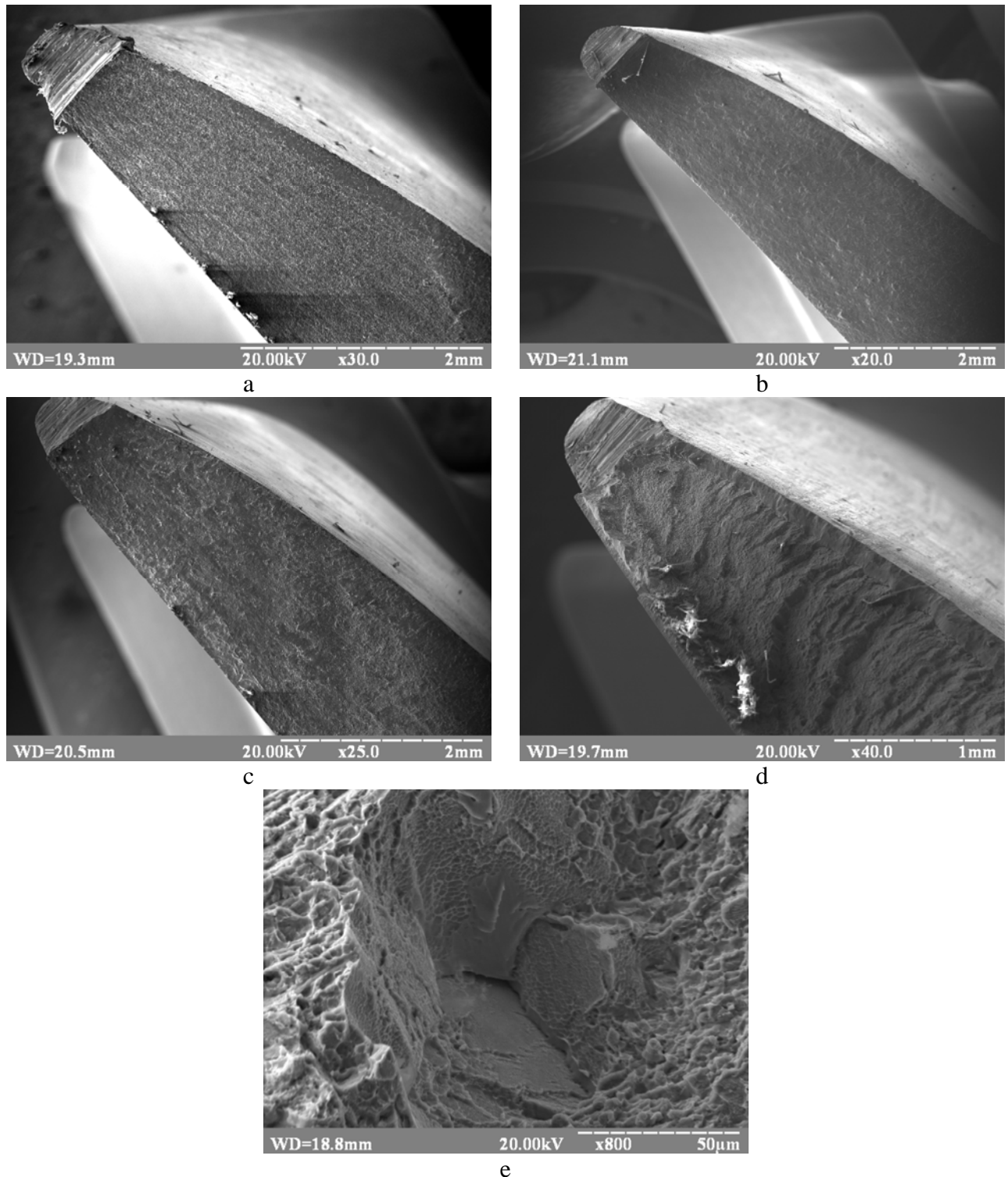
Fig. 45. Fracture surfaces of VT8 compressor blades fatigue tested with stress concentrators; conditions: (a) – initial; (b) – after LRHT/AC + aging; (c - e) – after LRHT/WQ + aging. SEM.

general view of fracture surfaces was approximately the same. At the same time if fracture was initiated from another but close to cut stress concentrator location (what was observed for LRHT/WQ + aged condition only!) fracture surface character was essentially different (compare Fig. 45d with Figs. 45a – c). Since number of fractured in such way blades was high we don't presented here obtained fatigue data, because them required special treatment and possibly additional study. However, it can assumed, that in case when LRHT was followed by water quenching obtained after final aging condition is characterized by too high strength, and stress concentrator forms on testing specific stress fields which caused in appearance of highest stresses in

another than cut concentrator location. This assumption may be confirmed by specific mode of fracturing crack propagation which illustrates even fracture through boundaries of separate grains (Figs. 45e), what indicates, that strength of material inside grain is higher than strength of grain boundary [11, 23].

By the way, obtained data unambiguously illustrates advantages of LRHT employment for improvement of fatigue properties of engine compressor blades made of two-phase α+β titanium alloy.

5. PRESENTATION AND PUBLICATION OF OBTAINED RESULTS

5.1. Obtained in project results were presented by project manager Dr. P. Markovsky on the following International Conferences:

1) "Materials and Coatings for Extreme Conditions: Research Studies, Application, Environment-Friendly Technologies of Production and Utilization", 22-26 September, 2008, Yalta, Ukraine;
2) "Titanium-2009 in CIS", Odessa, Ukraine, 17-20 May, 2009;
3) Processing and Fabrication of Advanced Materials "PFAM-XVIII", Tohoku University, Sendai, Japan, 13-16 December, 2009;
4) TMS Annual Meeting, Symposium "Cost affordable titanium alloys III", 15-18 February, 2010, Seattle, WA, USA,.

5.2. These results also were used for preparation of following published papers:

1) Markovsky P.E., Bondarchuk V.I., Matviychuk Yu. V., Microstructure and mechanical characteristics of VT1-0 alloy after surface rapid heat treatment, Material Science, 2008, v. 44, #3, pp.57-61.
2) Markovsky P.E., Local (Surface) Heat Treatment of Titanium Alloys: Microstructure and Mechanical Properties, In: Proceedings of the International symposium "Processing and Fabrication of Advanced Materials XVIII", 12-14 December 2009, Sendai, Japan, Tohoku University, V. 2, pp. 667-678.
3) Markovsky P.E. and Semiatin S.L., Microstructure and Mechanical Properties of Commercial-Purity Titanium after Rapid (Induction) Heat Treatment, Journal of Materials Processing Technology, 2010, 2010, v. 210, issue 3, pp. 518-528.
4) Markovsky P.E., Application of Local Rapid Heat Treatment for Improvement of Microstructure and Mechanical Properties of Titanium Products, Key Engineering Materials Vol. 436 (2010) pp 185-194.

One more paper with temporary title "Tailoring of Microstructure and Mechanical Properties of Ti-6Al-4V alloy with Local Rapid (Induction) Heat Treatment" is now under preparation.

6. CONCLUSIONS.

i) For executing of LRHT in cylindrical specimens as well as for real engine compressor blades a set of equipment based on electromagnetic induction generator (having frequency 400 kHz and maximum capacity 5 kW) was designed, produced, tested and showed a good efficiency.
ii) X-ray method for appeared during LRHT residual stresses evaluation was proposed and tested. Obtained for CP-Ti specimens data confirmed conclusion, that introduced by fast heating and cooling internal stresses are one of reasons (but minor) of mechanical properties increase.
iii) Combined experimental/calculation method was proposed and applied for evaluation of temperature distribution through Ø8mm CP-Ti, Ti-6-4 and TIMETAL-LCB specimens and real

compressor blade made of VT8 alloy appeared on LRHT.

iv) Different LRHT-treated conditions of CP-Ti were prepared, and tested as hardness through cross-section, tensile and fatigue properties. Obtained data was compared with initial and final annealed conditions. During LRHT comprising heating rates to 400°C/s and final water quenching, radial gradients in alpha-grain size, substructure/martensite, and residual stress are developed. This leads to improvements in strength and fatigue behavior with little-to-no effect on RA; only the tensile ductility is deleteriously affected. The principal strengthening mechanism associated with LRHT of CP-Ti was concluded to be the formation of substructure and martensite during rapid heating and cooling.

v) Investigation of LRHT influence on microstructure and tensile properties of Ti-6-4 with initial globular microstructure was done. It is established that balance of tensile strength and ductility after LRHT-hardening of this alloy looks rather attractive, although achieved level of strength is a little lower as compared with results of bulk RHT. It is supposed that reason of such decrease in tensile strength is difference in tensile straining of inner (softer) and outer (harder) layers, initiating rather earlier fracturing in transition between them zone, then cracking propagated to inner layers, and finished in outer layers. Also, it was found, that high-cycle fatigue of LRH-Treated Ti-6-4 is on the same highest level like after bulk RHT, whereas low-cycle fatigue (LCF) level was close to ones for initial condition. It was concluded, that reason of this easily propagation of fracturing cracks at higher applied stresses (LCF) in gradient microstructure in contrast to uniform one (formed on bulk RHT).

vi) For Ti-64 alloy having initial coarse-grained lamellar microstructure best result in mechanical properties improvement caused double LRHT application, that allows to refine intragrain α+β microstructure.

v) Possibility of LRHT employment to titanium β-alloy TIMETAL-LCB was studied and it was established, that refinement of surface layers via recrystallization during controlled on LRHT allows to obtain after final aging a good balance of strength and ductility.

vi) LRHT application to the turbine engine compressor blades showed possibility to form in critical section fine-grained beta-transformed microstructure which improved fatigue performance of these parts tested in usual (without stress concentrators) condition as well as after stress concentrators cutting.

vii) All researches were done in complete accordance with working plan.

7. LIST OF SYMBOLS, ABBREVIATIONS, AND ACRONYMS

1) CP-Ti – commercial purity titanium;
2) Ti-6-4 – titanium base alloy containing 6 weight % of aluminium and 4% of vanadium;
3) TIMETAl-LCB – titanium base beta alloy (low-cost) containing: 4.5 weight % of iron, 1.5 % of aluminium and 6.8% of molybdenum;
4) VT8 – titanium base alloy containing 6.7 weight %) aluminum and 2.9 % of molybdenum;
5) LRHT – Local (surface) Rapid Heat Treatment;
6) RHT – Rapid Heat Treatment;
7) Hz – hertz units, here – frequency of specimens' rotation during fatigue testing;
8) kWt – power of induction heating in kilowatts;
9) N sec – duration of LRHT in seconds;
10) LCF – low-cycle fatigue;
11) HCF – high-cycle fatigue;
12) WQ – water quenching;
13) AC – Air Cooling;
14) LM – Light Microscopy;
15) TEM – Transmission Electron Microscopy;
16) SEM – scanning electron microscopy.

8. REFERENCES.

[1] A.E. Slukhotsky, Application of High Frequency Current in Electrothermics, Mashinistroenie Publ., Leningrad, 1973, (in Russian).

[2] Generator for induction heating VChI-5, Technical description (in Russian), Institute for Electrodynamics, Kiev, 2005, 18 p.

[3] S.L. Semiatin and I.M. Sukonnik, Proc. of 7th International Symposium on Physical Simulation if Casting, Hot Rolling and Welding, ISPS, 21-23 Jan. 1997, pp. 395-405.

[4] Yu. A. Bagaryazky, ed., X-Ray Investigations in Physical Metallurgy, Metalurgizdat, Moscow, 1961, (in Russian).

[5] A. Taylor, X-Ray Metallography, John Willey & Sons, Inc. New York, 1961.

[6] A. Shiro, M. Nishida, T. Jing, Proc. of the 11th World Conference on Titanium, Kyoto, Japan, 3-7 June, 2007, Japan Institute of Metals, V.1, pp. 247-250.

[7] Krivoglaz M.A., 1996. X-Ray and Neutron Diffraction in Non-Ideal Crystals, Springer-Verlag, Berlin, 342 p.

[8] P. J. Withers, H. K. D. H. Bhadeshia, Mat. Sci. & Techn. 17 (4) (2001) 355.

[9] A.V. Lykov A.V. Theory of Thermal Conductivity, High School Publ., Moscow, 1967, (in Russian).

[10] Markovsky P.E., Pishchak V.K., Mordyuk B.M, Okrainets P.N., 2006. Improvement of fatigue characteristics of VT1-0 titanium alloy by surface mechanical and high-speed heat treatment, Materials Science, 42, 376-383.

[11] Lutjering G., 1998. Influence of processing on microstructure and mechanical properties of (α+β) titanium alloys, Material Science and Engineering, A243, 32- 45.

[12] Malinov S., Markovsky P.E., Sha W. et al., Resistivity study and modeling of the isothermal transformation kinetics of Ti-6-4 and Ti6242 titanium alloys, Journal of Alloys and Compounds, 2001, **314**, #1-2, pp. 181-191.

[13] Ivasishin O.M. and Markovsky P.E. Enhancing the Mechanical Properties of Titanium Alloys with Rapid Heat Treatment (Overview), JOM, 1996, #7, pp.48- 52.

[14] Peters J. O., Luetjering G., Ivasishin O.M. and Markovsky P.E., Mechanical Properties of Fine- Grained Beta-Titanium Alloys, In: Proc. Of 3rd Paris ASM Conf. On Synthesis, Processing and Modelling of Advanced Materials, 1997, pp. 269- 274.

[15] P.E. Markovsky, and M. Ikeda, Balancing of Mechanical Properties of Ti-4.5Fe-7.2Cr-3.0Al using Thermomechanical Processing and Rapid Heat Treatment, *Materials Transactions*, *JIM*, Vol.46 No.07 (2005) pp.1515-1524.

[16] O.M. Ivasishin, P.E. Markovsky, Yu.V. Matviychuk, S.L. Semiatin, C.H. Ward, and S. Fox, A comparative study of the mechanical properties of high-strength beta-titanium alloys, Journal of Alloys and Compounds, 2008, Volume 457, Issues 1-2, p. 296-309.

[17] Troshchenko V.T., Ivasishin O.M., Gryaznov B.A., Markovsky P.E., Strength of Materials, V. 27, Nos. 5-6, (1995), p.. 245-251.

[18] Mechanics of fracture and strength of materials, Reference book, V.V. Panasyuk Ed., Kiev, Naukova Dumka Publ., (in Ukrainian), v.4, 680 p.

[19] B.G. Belov, Ultrasonic and vibromagnetic treatment of metals, Metal Science and Heat Treatment, Volume 13, Number 3 / March, 1971, p. 261.

[20] Ivasishin O.M., Markovsky P.E., Dneprenko V.N. et al., Influence of thermomechanical and mechanical processing on the fatigue resistance of VT3-1, Strength of Materials, 1992, (2), pp.391-399.

[21] Ivasishin O.M., Markovsky P.E., Pakharenko G.A. and A.V.Shevchenko, Mechanical properties of (α+β) titanium alloys at cryogenic temperatures, Mat. Sci. & Eng., A196, 1995, pp.65-70.

[22] Ivasishin O.M., Markovsky P.E. et al., Effect of the cooling rate on the microstructure of titanium alloys heat hardened with incomplete β-phase homogenization, Phys. Metals, V.7(3), 1987, pp.508-520.

[23] Lutjering G., Ivasishin O.M., Albrecht J., Microstructure/properties relationships of titanium alloys, TMS, Warrendale, PA, 1994, pp. 65-74.

Project Manager

Pavlo E. Markovsky

Data: April 02, 2010